

Re-examining models of shallow-water deltas: Insights from tank experiments and field examples

Jutta Winsemann^{a,*}, Jörg Lang^a, Juan J. Fedele^b, Carlos Zavala^c, David C.J.D. Hoyal^b

^a Institut für Geologie, Leibniz Universität Hannover, Callinstraße 30, 30167 Hannover, Germany

^b ExxonMobil Upstream Research Company, 22777 Springwood Village Parkway, 77389 Spring, TX, USA

^c Departamento de Geología, Universidad Nacional del Sur, San Juan 670, Bahía Blanca B800 JUF3, Argentina

ARTICLE INFO

Article history:

Received 19 February 2021

Received in revised form 26 June 2021

Accepted 27 June 2021

Available online 5 July 2021

Editor: Dr. Catherine Chagué

Keywords:

Shallow-water deltas

Tank experiments

Bedforms

Supercritical flows

Pure jets

Stratified jets

Hyperpycnal flows

ABSTRACT

Shallow-water deltas remain enigmatic in terms of placing the observed facies within a coherent process-based depositional model. Here we report tank experiments on mouth-bar formation from shallow water pure and stratified jets that, combined with recent flume experiments on bedforms, suggest new interpretations of field observations from shallow-water delta outcrops.

Our experiments imply that the height, geometry and bedforms of the mouth bars depend on the jet properties and grain size of the supplied sediment. Pure jets with very coarse-grained sediment formed a high and steep mouth bar that is characterised by steep angle-of-repose cross bedding with related avalanche processes (grain flows) on the lee side. The experiments with stratified jets imply that mouth-bar deposition and growth are dominated by supercritical density flows that evolve from the initial jets on the lee side of the growing mouth bar. In stratified jets with very coarse-grained sediment, deposition on the mouth-bar lee side was both from grain-flow avalanches and density flows. While deposition on the upper lee slope was dominated by grain flows, a concentric field of low relief, asymmetric, downflow-migrating bedforms evolved on the lower slope and beyond the mouth bar. In the stratified jet with medium-grained sediment a very low relief mouth bar formed within a concentric field of low, asymmetric, downflow-migrating bedforms covering the entire lee slope and the area beyond.

Many previous field studies show that mouth bars deposited from dense stratified jets (hyperpycnal flows) are characterised by a distinct facies assemblage of coarse-grained cross-stratified or low-angle cross-stratified sandstone passing downslope into finer-grained plane-parallel, or “quasi-parallel” laminated sand and into climbing-ripple cross-laminated sandstone. Comparison to flume and tank experiments suggests that the proximal coarse-grained planar and trough cross-stratified sandstones could represent deposition by supercritical dunes that pass downslope into antidunes, characterised by sinusoidal stratification and/or low-angle cross stratification. The repeated vertical transition between antidune deposits and climbing-ripple cross-laminated sandstone may indicate the superposition of ripples onto antidunes in finer-grained sediments, indicating ripple formation under supercritical flow conditions. Similar bedforms/sedimentary structures have previously been interpreted as hummocky cross-stratification or swaley cross-stratification and attributed to combined flows in storm-dominated settings, which probably in some cases must be revised.

© 2021 The Author(s). Published by Elsevier B.V. This is an open access article under the CC BY license (<http://creativecommons.org/licenses/by/4.0/>).

1. Introduction

1.1. Objectives

Bedforms related to supercritical flows are increasingly recognised in steep (Gilbert-type) deltas and fan deltas and have been identified as important constituents of these depositional environments (e.g., Massari, 1996; Dietrich et al., 2016; Hughes Clarke, 2016; Lang et al., 2017b, 2021b; Massari, 2017; Winsemann et al., 2018; Postma

et al., 2021; Tan and Plink-Björklund, 2021). In contrast, deposits of supercritical flows in shallow-water mouth-bar deltas have neither received much attention, nor have they been widely considered in current sedimentological models. Previous field-based studies focussed mainly on the morphology and larger-scale depositional architecture of shallow-water deltas (e.g., Postma, 1995; Olariu and Bhattacharya, 2006; Zavala et al., 2006; Fielding, 2010; Schomacker et al., 2010; Jerrett et al., 2016; Winsemann et al., 2018; Cole et al., 2021). Frequently described sedimentary structures of mouth-bar deposits are high- to low-angle cross-stratification, plane-parallel or “quasi-parallel”-lamination, climbing-ripple cross-lamination as well as hummocky cross-stratification (HCS) and swaley cross-stratification (SCS), mainly

* Corresponding author.

E-mail address: winsemann@geowi.uni-hannover.de (J. Winsemann).

attributed to subcritical flows, oscillatory flows and/or combined flows (e.g., Mutti et al., 1996, 2000; Zavala et al., 2006; Ahmed et al., 2014; Cole et al., 2021; Lin and Bhattacharya, 2021).

However, many studies on bedforms and sedimentary structures deposited from supercritical flows (e.g., Alexander et al., 2001; Fielding, 2006; Lang and Winsemann, 2013; Cartigny et al., 2014; Lang et al., 2017a, 2017b, 2021a, 2021b; Massari, 2017; Vaucher et al., 2018; Slootman and Cartigny, 2020; Ono et al., 2021; Postma et al., 2021; Slootman et al., 2021; Tan and Plink-Björklund, 2021) indicate that these bedforms/sedimentary structures may partly resemble hummocky cross-stratification (HCS) and swaley cross-stratification (SCS). Previous interpretations of HCS- and SCS-like structures therefore may need to be reconsidered.

Here, we compare results of tank experiments to field examples of marine and lacustrine shallow-water deltas. We discuss i) the wider implications of mouth-bar growth and the lateral and vertical facies evolution of coarse-grained shallow-water delta systems; ii) the hypothesis that concentric fields of low relief, asymmetric, downflow-migrating bedforms that formed on the lee slope of coarse-grained shallow-water mouth bars in tank experiments represent supercritical bedforms of dunes and antidunes; iii) that current-ripple formation took place on the stoss-sides of antidunes under supercritical flow conditions and iv) that previous interpretations of HCS- and SCS-like structures may partly have to be revised and these bedforms instead may represent deposits of stable and breaking antidunes and/or chutes-and-pools.

1.2. Background

1.2.1. Characteristics of shallow-water deltas

Shallow-water deltas are constructive depositional elements that develop when a river enters in a marine or lacustrine basin. Shallow-water deltas deposited on low gradient basin margins commonly have a gently inclined profile and comprise three physiographic zones (Nemec, 1990; Postma, 1990): the delta plain, comprising the alluvial feeder system; the delta front dominated by deposition of the coarse-grained bed load; and the prodelta, dominated by suspension fallout from deltaic buoyant plumes.

Feeder systems of coarse-grained shallow-water deltas are often composed of moderate- to low-gradient gravelly and sandy alluvial systems and glacial outwash plains (e.g., Postma, 1990; Mutti et al., 1996, 2000; Leren et al., 2010). So-called braid (-plain) deltas form where braided rivers or glaciofluvial outwash plains (sandurs) prograde into a standing water body (e.g., Nemec, 1990; Postma, 1990; MacNaughton et al., 1997; Tuttle et al., 1997). They are the common delta style in hot semiarid, glacial and pre-vegetation systems (e.g., McPherson et al., 1987; Eriksson et al., 1998; Muhlbauer and Fedo, 2020; Went, 2020).

Mouth bars form in front of relatively stable feeder channels, where the lateral dispersion of sediment is confined to a narrow zone. The width of mouth bars depends on the spreading angle of the expanding jet. Flume, tank and numerical models have considerably increased the understanding of mouth-bar formation and its response to allogenic forcing and autogenic dynamics (Bates, 1953; Wright, 1977; Hoyal et al., 2003; Overeem et al., 2005; Wellner et al., 2005; Edmonds and Slingerland, 2007; Rowland et al., 2009; Fagherazzi et al., 2015; Piliouras et al., 2017; Daniiller-Varghese et al., 2020; Lang et al., 2021a). Mouth bars may pass basinward into delta-front lobes and fine-grained prodelta sediments. If feeder channels are closely spaced, bars will coalesce to create a uniform delta front (e.g., Nemec, 1990; Postma, 1990; Mutti et al., 1996, 2000, 2003; Surlyk and Bruhn, 2020).

The morphology, depositional architecture, and facies assemblage of shallow-water deltas are controlled by the available accommodation space, water discharge as well as the rate, grain size, and amount of sediment supply, which in turn are controlled by tectonics, lake- or sea-level change and climate (Postma, 1990, 1995; Olariu and Bhattacharya, 2006; Fielding, 2010; Martins-Neto and Catuneanu,

2010; Olariu et al., 2010; Schomacker et al., 2010; Gobo et al., 2014; Ambrosetti et al., 2017; Winsemann et al., 2018; Van Yperen et al., 2020; Cole et al., 2021; Melstrom and Birgenheier, 2021). In low accommodation settings, shallow-water deltas may be only a few metres thick with a gently inclined delta front and an overall subhorizontal bedding geometry. The depositional dips of clinofolds have average values of 1 to 5° and maximum values of 10 to 15° (Dunne and Hempton, 1984; Tye and Coleman, 1989; Nemec, 1990; Postma, 1990; Zavala et al., 2006; Olariu et al., 2010, 2020; Ambrosetti et al., 2017; Winsemann et al., 2018). The deposition may be dominated by friction- and/or inertia-dominated jets and reworking by waves and tides may occur (Wright, 1977; Postma, 1990; Fidolini and Ghinassi, 2016; Jerrett et al., 2016; Kurcinka et al., 2018; Li et al., 2018; Lin and Bhattacharya, 2021). In higher accommodation settings, shallow-water deltas may be deposited during slow rises of base-level on top of Gilbert-type deltas (Ilgar and Nemec, 2005; Mortimer et al., 2005; García-García et al., 2006; Ghinassi, 2007; Rajchl et al., 2008; Ambrosetti et al., 2017) or overlies/onlap Gilbert-type deltas and subaqueous (ice-contact) fans during rapid base-level falls (e.g., Chough and Hwang, 1997; Sohn and Son, 2004; Winsemann et al., 2009, 2018). In settings characterised by rapid base-level rise shallow-water deltas may evolve into Gilbert-type deltas (e.g., Hwang et al., 1995; Ilgar and Nemec, 2005; García-García et al., 2006; Gobo et al., 2014).

Many ancient shallow-water delta deposits form prolific hydrocarbon and freshwater reservoirs in the subsurface. In recent years lacustrine shallow-water delta sandstones have also become one of the most important targets for exploration (McPherson et al., 1987; Liangqing and Galloway, 1991; Zavala et al., 2006; Ambrosetti et al., 2017; Zhu et al., 2017; Olariu et al., 2020; Zavala, 2020; Cole et al., 2021).

1.2.2. Deposition of shallow-water mouth bars from pure and stratified jets

Shallow-water mouth bars are deposited when a confined river expands and decelerates into a standing body of water. Flow behaviour upon the loss of the lateral confinement can be modelled as a wall jet. Jets are typically momentum-dominated and evolve into gravity-dominated flows by dissipation of the initial momentum due to the development of large-scale turbulence (Bates, 1953; Wright, 1977; List, 1982; Powell, 1990). Wall jets are bounded by a wall, e.g., the bed or the water surface, causing increased friction and thus deceleration of the jet (Wright, 1977; Powell, 1990). At very shallow water depths, jets may be bounded by both the bed and the water surface. Additional parameters that control the jet behaviour include orifice diameter, discharge, flow velocity at the orifice and density contrast with the ambient water (Powell, 1990; Hoyal et al., 2003; Lang et al., 2021a). Jets with the same density as the ambient water are termed pure jets, while jets with a density contrast are termed stratified or buoyant jets (Ellison and Turner, 1959; Chu and Baddour, 1984; Jirka, 2004). The term stratified jet (or stratified flow), however, is not supposed to imply a stratification due to density differences within the flow but refers solely to the density contrast with the ambient water. Density contrasts with the ambient water may be negative or positive due to salinity, sediment load or temperature. As the jet expands into the basin, its overall velocity decreases. At locations where the flow velocity is below the critical threshold for sediment mobility, jets deposit their sediment load. These jet deposits commonly display a proximal to distal zonation with a distinct downflow and lateral grain-size decay (Wright, 1977; Hoyal et al., 2003; Wellner et al., 2005; Edmonds and Slingerland, 2007; Daniiller-Varghese et al., 2020; Lang et al., 2021a).

In coarse-grained shallow-water deltas, friction-dominated and inertia-dominated jets prevail. Friction-dominated jets are common in settings where the depth of the basin downstream of the channel outlet is similar or shallower than the channel depth itself (Wright, 1977). These flows decelerate rapidly and expand laterally due to bed friction and turbulent jet diffusion, resulting in the deposition of a coarse-grained mouth bar. Internally these mouth bars are characterised by steep angle-of-repose cross bedding with related avalanche processes

(grain flows) on the lee side (e.g., Wright, 1977; Ahmed et al., 2014; Fidolini and Ghinassi, 2016; Winsemann et al., 2018; Cole et al., 2021). Inertia-dominated jets are common in settings where the depth of the basin downstream of the channel outlet is deeper than the channel depth itself (Wright, 1977).

Downflow, momentum-dominated stratified jets will evolve into gravity-dominated density flows. The evolution of the gravity-dominated flow is controlled by its initial momentum and its density contrast. In the so-called near field close to the river mouth, inertia and mixing processes are controlled by the discharge and density of the jet. Further downslope, the effect of density differences between the expanding jet and the ambient water becomes increasingly important as inertia decays and the flow evolves into a density flow in the so-called far field, controlled by gravity and buoyancy forces (Roberts et al., 2001; Lang et al., 2021a). Hydraulic jumps are absent in submerged 3D wall jets due to free flow expansion and transformation. Flow transformation in 3D wall jets is different from density flows with a free interface and includes complex recirculation, pulsating bursts and waves, and flow splitting within the scour (Ade and Rajaratnam, 1998; Lang et al., 2021a). If the initial density of the stratified jet is higher than the density of the ambient water, hyperpycnal flows will form that are able to transport sediment further into the basin (Powell, 1990; Mutti et al., 2000; Zavala et al., 2006; Surlyk and Bruhn, 2020; Zavala, 2020; Lang et al., 2021a). Development of hyperpycnal flows may be enhanced by sediment settling due to decreasing jet-related turbulence (Powell, 1990; Dowdeswell et al., 2015). Formation of hyperpycnal flows is especially common in freshwater lakes because of the lower density of the water in the reservoir (e.g., Bates, 1953; Mulder et al., 2003; Zavala et al., 2006; Winsemann et al., 2009, 2018; Zavala, 2020). In marine settings, the formation of hyperpycnal flows is commonly attributed to highly concentrated (sediment-laden) flood events, such as flash-floods in hot semiarid environments or jökulhlaups in glacial environments (Mutti et al., 1996, 2000; Mulder et al., 2003; Ghiene et al., 2010; Girard et al., 2012; Lang et al., 2012, 2021a, 2021b; Jin et al., 2021). However, hyperpycnal flows may also evolve from relatively low sediment-loads due to settling from buoyant plumes (Parsons et al., 2001; Hage et al., 2019). Coarse-grained hyperpycnal flow deposits are characteristic of glacial settings and smaller river systems in steeper terrains of tectonically active basins (Mutti et al., 2000; Uličný, 2001; Mulder et al., 2003; Cao et al., 2018; Winsemann et al., 2018).

2. Dataset and methods

2.1. Tank experiments

2.1.1. Setup of the experiments

3D tank experiments with submerged wall jets were conducted in the Sedimentology and Stratigraphy Experimental Facility at ExxonMobil Upstream Research Company (Houston, Texas, USA). The experimental setup comprises an 8 m long and 5 m wide plate placed

in a 10 m long, 7 m wide and 2 m deep glass-walled tank filled with tap water. The slope of the plate was fixed at 10° . A system comprising a Venturi pipe and external feeder for sediment and salt was used to combine desired water, sediment and salt discharge rates. Water, salt and sediment were mixed through the Venturi pipe and pumped to a head tank, providing the capability of generating steady, long duration flows (Fig. 1).

The jets were released from a pipe with diameters of 5.08 cm mounted to the plate. Accordingly, the axis of the pipe was half the pipe diameter above the surface of the bed. The water level in the tank was adjusted to the upper rim of the pipe and kept constant during the experiments. The set-up included slow feed of fresh water and slow drain of the accumulated denser fluid from the bottom of the tank during the runs. An additional tank storage volume at the downflow end and lateral sides prevented build-up of stratified fluid to the level of the outflow at the end of the plate. Dye was added to allow for the visual observation of the flows.

Stratified, dense jets were produced using a brine solution of constant density by mixing water and salt in the Venturi in-line mixing system, while for experiments with pure jets (non-stratified) no salt was added. The sediment used in the experiments is a crushed melamine plastic with a density of 1.57 g cm^{-3} , which is supplied in sieved uniform mixtures of fine (0.149–0.177 mm), medium (0.177–0.25 mm) and very coarse (0.59–0.84 mm) grains. The sediment fed into the flows was either medium-grained or very coarse-grained. Mixtures of different grain sizes were not used. The prepared flat sediment bed consisted of fine-grained sediment of the same material with a bed thickness of $\sim 5 \text{ cm}$.

Due to the low water depths near the inlet pipe in the upper part of the tank, it was not possible to measure the velocity and density of the flows during the experiments. However, analogies can be drawn from measurements conducted in the same tank with the same experimental set-up but deeper submergence of the inlet pipe (cf., Lang et al., 2021a).

2.1.2. Conducted experiments

3 runs (A–C) of shallow water aggrading jets, expanding on an inclined (10°) erodible bed were conducted (Table 1; Figs. 2, 3; Supplementary data 1, 2). Jets were released from a pipe with a constant discharge of 0.44 l/s . Both pure and stratified jets were tested. The stratified jets had a density of 1.06 kg l^{-1} at the outlet, corresponding to a fractional density difference ($\Delta\rho/\rho$) of 0.06. The corresponding densimetric Froude numbers (Fr') at the outlet are ~ 1.6 for the stratified jets (runs B and C) and approaching infinity for the pure jet (run A). It should be noted that the densimetric Froude number has no physical meaning in the near field of jets issuing from closed pipes due to the lack of a free flow interface (Lang et al., 2021a). However, the (densimetric) Froude number is a convenient and widely applied parameter, making the jet conditions easier to compare to flows issuing from subaerial or submerged channels. Sediment was fed into the flows at constant rates of 8.3 g s^{-1} for very coarse-grained sediments (runs A and B) and 8.4 g s^{-1} for medium-grained sediments (run C).

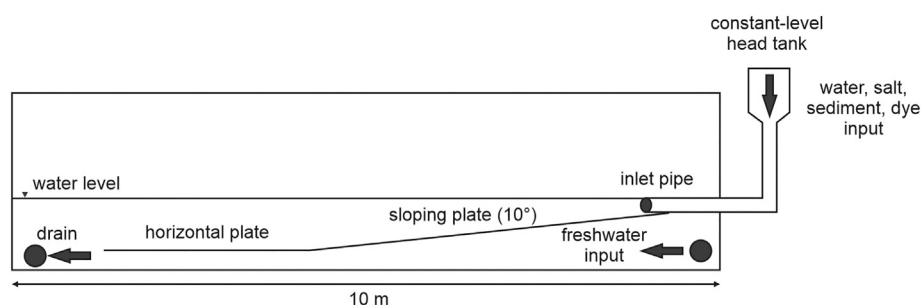
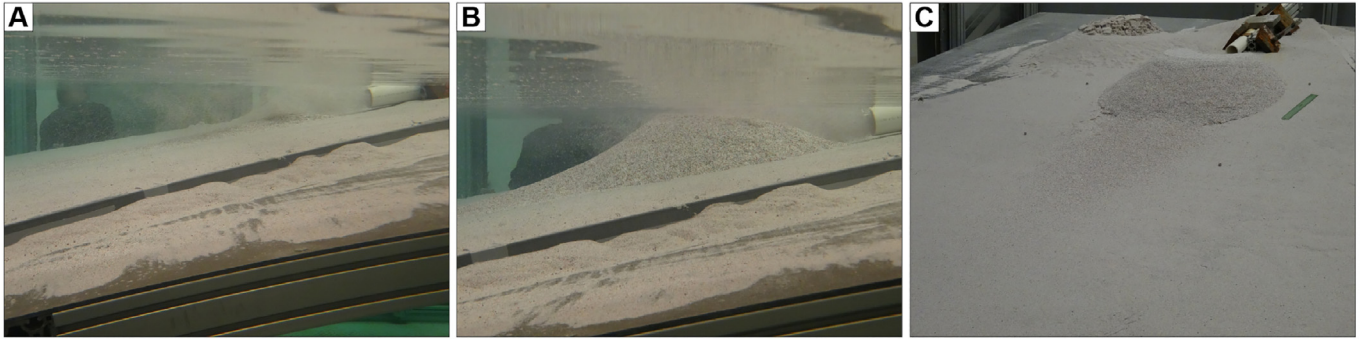


Fig. 1. Cross-sectional view of the experimental set-up. The width of the tank is 7 m. The inlet pipe is placed in the centre of a 5 m wide plate.

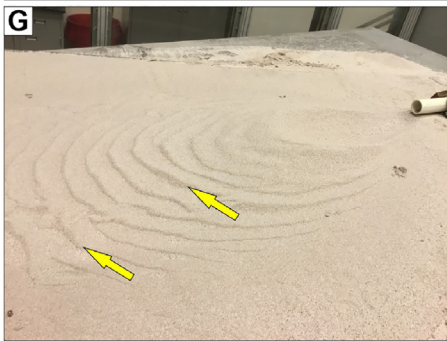
Run A (pure jet)



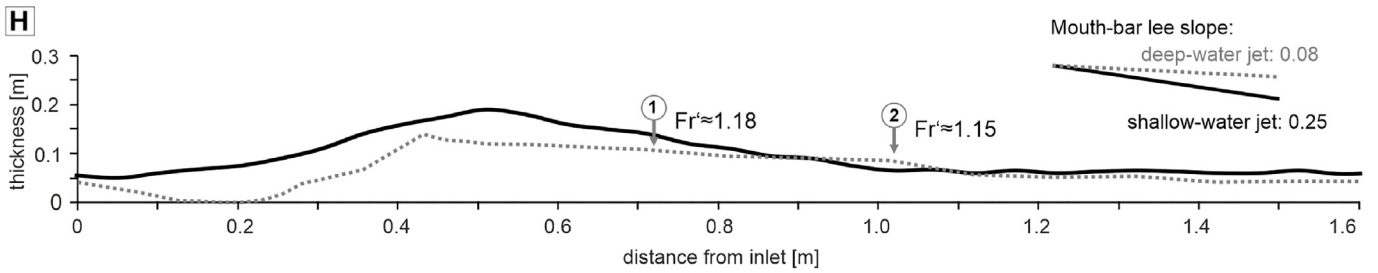
Run B and C (stratified jets)



Formation of low-relief asymmetric bedforms on the lower slope of the mouth bar and beyond

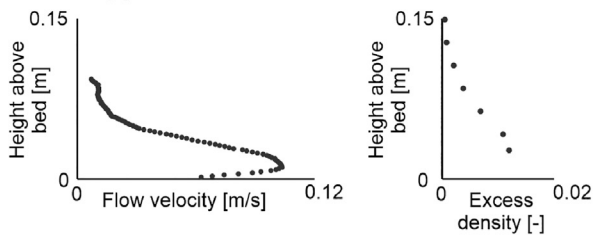


Formation of low-relief asymmetric bedforms on the entire slope of the mouth bar and beyond

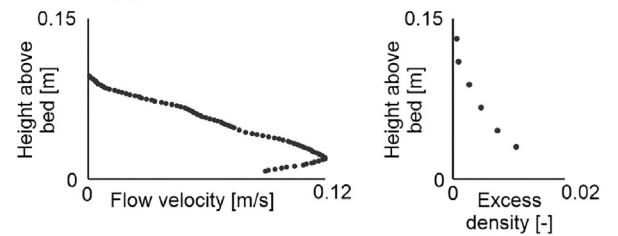


Measurements from deep-water jets

Measuring point 1



Measuring point 2



2.2. Field data

Outcrop data were studied to reconstruct the sedimentary facies and depositional processes of shallow-water delta systems. The dataset consists of outcrop descriptions from various marine and lacustrine shallow-water deltas and comprises data from our own field work and published field examples from the literature. The selected field examples are considered to be representative of delta styles in different shallow-water settings. Outcrop descriptions include data on grain size, sorting, roundness, sedimentary structures and bed geometry. The terminology for gravel characteristics is after Walker (1975). The fabric notation uses symbols a and b for the clast long and intermediate axes, with indices (t) and (p) denoting axis orientation transverse or parallel to flow direction, and index (i) denoting axis imbrication.

3. Results and interpretation

3.1. Tank experiments

The sediment supplied to the pure and stratified jets was transported in the pipe as both bed load and suspended load. At the orifice, the wall jets expanded by turbulent mixing with the ambient water at the flow interfaces. In pure jets, flow deceleration and expansion resulted in dissipation of jet momentum and complete mixing with the ambient water. Stratified jets evolved further basinwards into gravity-driven density flows (Fig. 2; Supplementary data 1, 2).

Jet expansion led to rapid deposition and the growth of a mouth bar. Some scouring of the sediment bed and re-entrainment of the deposited sediment occurred due to jet impingement, leading to the formation of bowl-shaped depressions (scours) at the stoss side of the mouth bars. However, the experimental jets were always net-depositional, and aggradation occurred also on the stoss sides of the mouth bars.

Initial mouth-bar growth occurred from vertical aggradation with a bi-directional dip of the depositional surface and was followed by lateral expansion and vertical accretion. The stoss sides of mouth bars were affected by intense turbulence of the incoming jets, causing constant remobilisation of sediment. Fine-grained sediment was transported to the lee side of the mouth bars by saltation and as suspended load, allowing the formation of bedforms. Coarse-grained sediment passing over the rim of the growing mouth bar favoured the generation of grain flows on its lee side. Grain flows were shed in all directions from the mouth-bar rim, with the largest part of the sediment being transported in the direction down-dip of the orifice. Suspended sediment was transported further basinwards.

3.1.1. Deposition from a sediment-laden pure jet (run A)

In experiments conducted with a pure jet (Tables 1, 2; Figs. 2A, B, C, 3A, D; Supplementary data 1) mouth-bar growth was very rapid due to flow deceleration and expansion, leading to the aggradation of the mouth bar to ~2 cm below the water level. The steep mouth-bar lee side was maintained by constant avalanching of sediment over the rim. Some sediment was transported over the growing mouth bar, forming a thin elongate sheet-like deposit at the distal end of the mouth bar (Figs. 2C, 3A). During the later stage of mouth-bar growth, the flow was no longer able to transport sediment over the mouth bar

due to the very low water depth remaining above the mouth bar. This change in sediment transport led to increased avalanching from the mouth-bar rim, causing a change of the geometry of the mouth-bar slope from convex-up to concave-up and the progradation of the mouth bar over the sheet-like deposit at its distal end (Fig. 2B). Bedforms on the mouth-bar lee side or the slope beyond were not observed in the pure jet experiment.

3.1.1.1. Interpretation. In the experiment with the pure jet, the flow and sediment dynamics were controlled by rapid dissipation of the jet due to mixing with the ambient water and consequent flow expansion. Pure jets are able to entrain ambient water faster than stratified jets due to the lack of a density contrast that hinders mixing (Fischer et al., 1979; Turner, 1986). The initial momentum of the jet is dissipated, and secondary gravity-driven flows cannot form (Hoyal et al., 2003; Lang et al., 2021a). Sediment transported by the incoming jet is therefore completely deposited at the mouth bar. Sediment transport in the early stage of the experiment was characterised by bed load and suspended load and/or saltation (Fig. 2A, B; Supplementary data 1). Bed load was deposited immediately in front of the orifice, leading to the rapid mouth-bar growth. The sheet-like deposit at the distal end of the mouth bar was formed by the sediment transported in suspension or by saltation. Mouth-bar growth limited the ability of the flow to bypass the mouth bar as the available water depth was successively lowered. In this stage, mouth-bar growth continued by avalanching at the front and sides of the mouth bar. Grain flows were fed from sediment that spilled over the rim of the growing mouth bar. The distal and lateral mouth-bar slopes were constantly kept at the angle of repose. Continuous mouth-bar growth led to an increase in avalanching on the lateral slopes due to the shorter transport distance compared with the frontal slope. Previous experiments with shallow (Daniller-Varghese et al., 2020) or deep water (Hamilton et al., 2015, 2017) mouth bars showed that at some stage flow splitting around the mouth bar occurred. The absence of flow splitting in our experiments is caused by the huge amount of accommodation space available on the steep basin slope and the fixed position of the entry point of the jet.

3.1.2. Deposition from sediment-laden stratified jets (run B and C)

In experiments with stratified jets, mouth-bar growth was less rapid and the mouth bars remained lower than the mouth bar in the pure jet experiment (Tables 1, 2; Figs. 2D, E, F, G, 3B, C, E, F; Supplementary data 2) The transition from jets to density flows occurred approximately at the mouth-bar crest. Negligible jet momentum remained in the decelerated flow, which was pushed over the mouth-bar crest by the incoming jet. A density flow formed on the lee side of the mouth bar due to the excess density of the flow and was accelerated by the imposed bed slope and the slope of the mouth bar. The density flow caused the formation of bedforms on the lower slope of the mouth bar and on the sediment bed further downslope.

Heights and geometries of mouth bars depended on the grain size of the supplied sediment. Very coarse-grained sediment led to the formation of an elongate, rounded mouth-bar (Figs. 2F, 3B, E). Deposition on the mouth-bar lee side was from grain flows and density flows, allowing the downslope extension of the mouth bar (Supplementary data 2). The mouth bar had a sharp downslope termination with almost no sediment

Fig. 2. Photographs of jet deposits. A–C) Pure jet with very coarse-grained sediment (run A). A) Early mouth-bar growth. Sediment is still able to bypass the mouth bar and is deposited as a thin sheet in front of the mouth bar. B) Late mouth-bar growth. Only few grains are still overpassing the mouth bar. Mouth-bar growth is mainly due to avalanching. C) Oblique view of the final mouth bar. The sheet-like deposit in front of the mouth bar is related to the overpassing sediments. D–F) Stratified jet with very coarse-grained sediment (run B). D) Formation of a density flow on the lee side of the mouth bar. E) Growing mouth bar with a rounded geometry and relatively low lee-side slope. F) Oblique view of the final deposit formed during run B. Note that low asymmetric bedforms have formed on the lower slope of the mouth bar and in fine-grained bed material beyond the mouth bar. These bedforms are interpreted as supercritical dunes and/or downstream migrating antidunes. G) Oblique view of the final deposit formed by a stratified jet with medium-grained sediment (run C). Low asymmetric bedforms have formed on the slope of the mouth bar and are interpreted as supercritical dunes and/or downstream migrating antidunes. The finer grain size compared with run B allowed for more extensive bedform formation. H) Comparison of thickness profiles of mouth bars from a shallow-water jet (black solid line, run B) and a deep-water jet (grey dashed line). For the deep-water jet measurements of the flow velocity and excess density and estimates of the densimetric Froude number Fr' are provided for two locations (modified after Lang et al., 2021a).

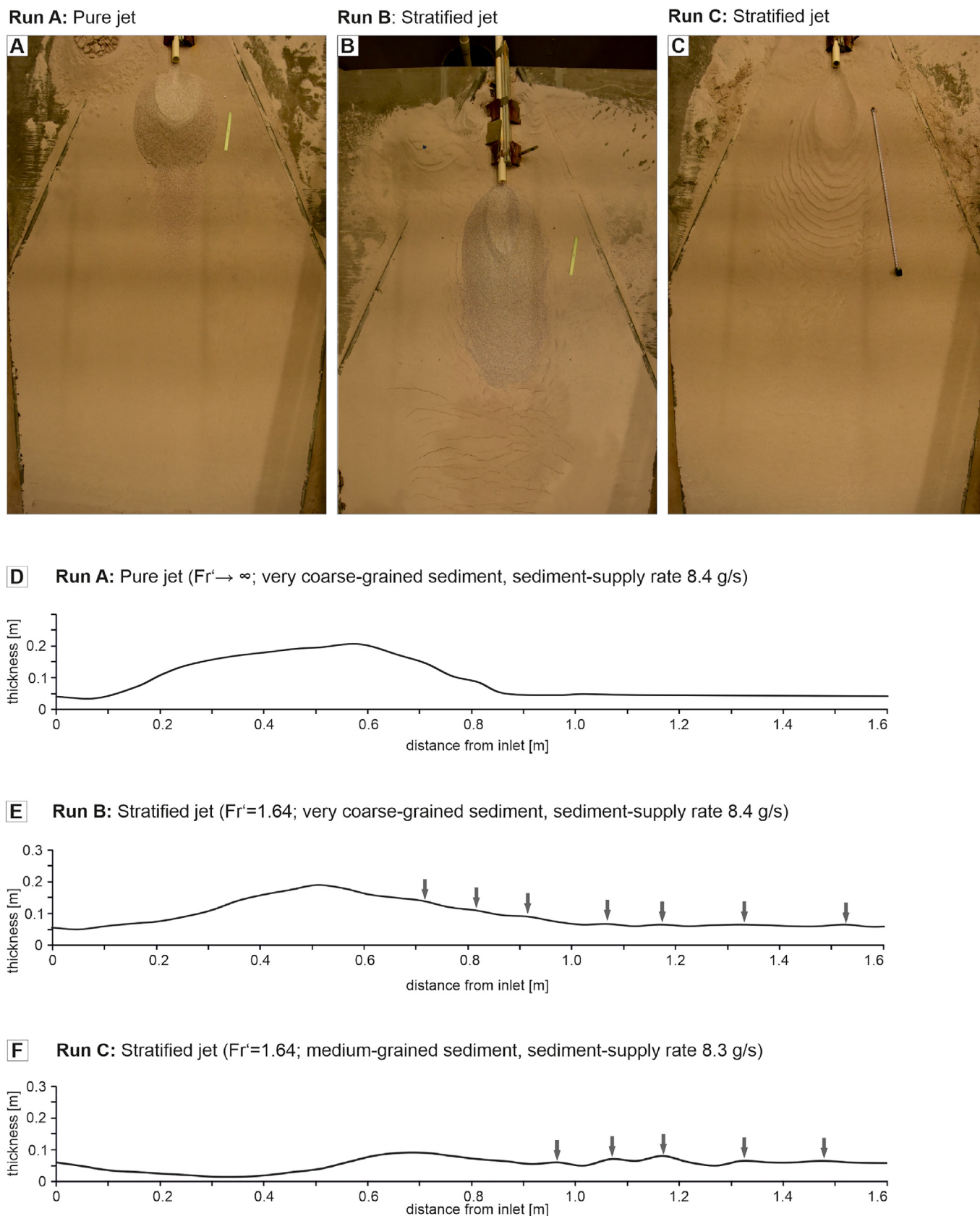


Fig. 3. Characteristics of mouth bars deposited by the experimental jets. A) Plan view of the final deposits formed during run A (pure jet, very coarse-grained sediment). B) Plan view of the final deposit formed during run B (stratified jet, very coarse-grained sediment). C) Plan view of the final deposit formed during run C (stratified jet, medium-grained sediment). D–F) Thickness profiles of the experimental jet deposits measured along the axis of the jet. Arrows indicate crests of low-relief bedforms superimposed on the mouth-bar lee side and beyond the mouth bars.

Table 1
Parameters of the conducted experiments.

Run #	Pipe diameter (cm)	Bed slope (°)	Outlet conditions				Sediment bed and supply		
			Discharge (l/s)	Flow velocity (m/s)	Fractional density difference $\Delta\rho/\rho$	Densimetric Froude number	Sediment bed	Sediment-supply rate (g s^{-1})	Supplied grain size
Run A	5.08	10	0.44	0.22	Pure jet	∞	~5 cm, fine-grained	8.4	Very coarse-grained
Run B	5.08	10	0.44	0.22	0.035	1.64	~5 cm, fine-grained	8.4	Very coarse-grained
Run C	5.08	10	0.44	0.22	0.035	1.64	~5 cm, fine-grained	8.3	Medium-grained

being transport further downslope. On the lower part of the mouth-bar lee side a concentric field of low, asymmetric, downflow-migrating bedforms evolved. Bedforms were 0.5 cm high, had wavelengths of 10 cm and slightly steeper lee than stoss sides. The bedform field continued downslope of the mouth-bar termination with bedforms consisting exclusively of (fine-grained) sediment derived from the bed (Figs. 2F, 3B, E).

Medium-grained sediment led to the formation of a very low relief mouth bar, lacking the broad lee slope observed in our other experiments (Figs. 2G, 3C, F). From the lee-slope of the mouth bar there was a smooth transition into a concentric field of low, asymmetric, downflow-migrating bedforms. The bedforms were 1.5 cm high, had wavelengths of 10–15 cm and steeper lee than stoss sides (Figs. 2G, 3C, F). Bedforms comprised both the medium-grained sediment fed into the jet and fine-grained sediment derived from the bed.

3.1.2.1. Interpretation. In the experiments with stratified jets, mouth-bar deposition was affected by the formation of a gravity-controlled density flow (Supplementary data 2). Density flows allow the sediment to be transported further into the basin, which is commonly associated with the formation of bedforms on the lower slope of the mouth bar and beyond. The grain size is a further controlling factor for mouth-bar growth. Finer grained sediment is transported by the density flow for longer distances, resulting in the formation of lower mouth bars and more extensive bedform fields downslope of the mouth bars. Bedforms observed both on the lower mouth-bar slope and on the sediment further downslope, displaying different geometries. In the absence of flow measurements, the interpretation of the bedforms must be based on their geometries, observations of the flow during the run and comparison to deep-water jet experiments under similar conditions (Lang et al., 2021a).

The observed proximal asymmetrical bedforms are interpreted as representing small-scale dunes, based on their asymmetrical geometry, downflow migration, the visually observed interactions of the bedforms and the flows aided by dye injection, and scaling estimates between bedform wavelength and flow thickness. Sediment was deposited on their lee sides by small-scale eddies. Downflow changes in bedform geometry and lateral continuity are probably related to velocity decay. The low-relief bedforms that evolved on the lower mouth-bar slope or beyond the mouth bar are interpreted as downstream migrating antidunes (cf., Fedele et al., 2016).

Mouth bars deposited by shallow-water jets are higher and have steeper lee side slopes than those deposited by deep-water jets under otherwise similar conditions (i.e., bed slope, grain size, initial flow

Table 2
Dimensions and aspect ratios of scour-mouth-bar pairs.

		Length (cm)	Width (cm)	Aspect ratio (L/W)
Run A	Scour	25.4	21.59	1.18
	Mouth bar	83.82	35.56	2.36
Run B	Scour	53.34	24.13	2.21
	Mouth bar	101.6	66.04	1.54
Run C	Scour	68.58	36.83	1.86
	Mouth bar	88.9	53.34	1.67

density) (Fig. 2H). The mouth bar formed in run B is approximately 3 times steeper (0.25 versus 0.08) than the mouth bar of the deep-water jet experiment of Lang et al. (2021a). Estimates of the densimetric Froude number for density flows on the mouth-bar lee sides by Lang et al. (2021a) suggest that flows by deep-water jets produced under the same experimental conditions are slightly supercritical on the lee slope of the mouth-bars (Fig. 2H). As the acceleration of the density flow on the steeper mouth-bar lee sides of shallow water jets will be higher it is likely that these density flows also attain supercritical conditions. Therefore, by analogy to Lang et al. (2021a), the asymmetrical bedforms are interpreted to represent supercritical dunes. This also conforms with further experiments by Fedele et al. (2016), who demonstrated that downslope migrating asymmetrical dune-scale bedforms deposited by saline density flows generally require Froude supercritical flows. Furthermore, Fedele et al. (2016) showed that the bedform height of supercritical dunes is considerably higher than that of the antidunes. The low-relief bedforms that evolved basinwards of the mouth-bar therefore most probably represent antidunes.

3.2. Examination of field examples

Two basic types of coarse-grained mouth-bar deposits are commonly reported from field examples that differ in depositional processes and the resulting facies architecture. These are i) mouth-bars dominated by avalanche and grain-flow processes and ii) mouth bars dominated by tractional bedforms (Figs. 4, 5, 6, 7).

3.2.1. Mouth bars dominated by avalanche and grain-flow processes

Mouth bars deposited by avalanche and grain-flow processes are characterised by steep sandy or gravelly foresets. The foresets may downlap sharply on the underlying deposits or transition tangentially into thin, a few cm-thick, finer-grained bottomsets that resulted from deposition of the suspended load (Figs. 4A, B, C, 7A, B, D). Up-flow, foreset beds may pass into subhorizontally stratified sandy topsets (e.g., Rajchl et al., 2008; Winsemann et al., 2009, 2018; Cole et al., 2021). Individual foreset beds are cm-dm thick and massive, inversely, normally and/or laterally graded. Bed contacts in gravelly mouth bars are uneven and partly erosional (e.g., Mutti et al., 1996, 2000; Ilgar and Nemeč, 2005; Winsemann et al., 2018). Long axes of outsized clasts may be aligned parallel to the dip of bedding planes, showing an a(p) a (i) fabric, indicating slide processes. Clast imbrication with an upslope-dipping a(t) b(i) fabric results from downslope rolling. Clast-supported open-work gravel lenses close to the foreset toe result from collapse of the steep upper mouth-bar slope and downslope movement of grains as avalanches (e.g., Nemeč et al., 1999; Rajchl et al., 2008; Winsemann et al., 2018). These open-work gravel lenses typically display a vertical normal grading and a lateral grading of a coarse head down-dip into an upslope fining tail. Coarser sand(stone) beds are commonly massive, inversely or normally graded and may show pin-stripe stratification (Figs. 4B, C, 7D) (e.g., Mutti et al., 1996, 2000; Ilgar and Nemeč, 2005; Rajchl et al., 2008; Winsemann et al., 2009; Cole et al., 2021). Intercalated finer-grained sand and silt beds may show (partly upslope) climbing-ripple cross-lamination indicating deposition from hyperpycnal flows. Massive sand(stones) or gravelly and sandy backsets filling spoon-shaped scours in the stoss and lee side deposits of

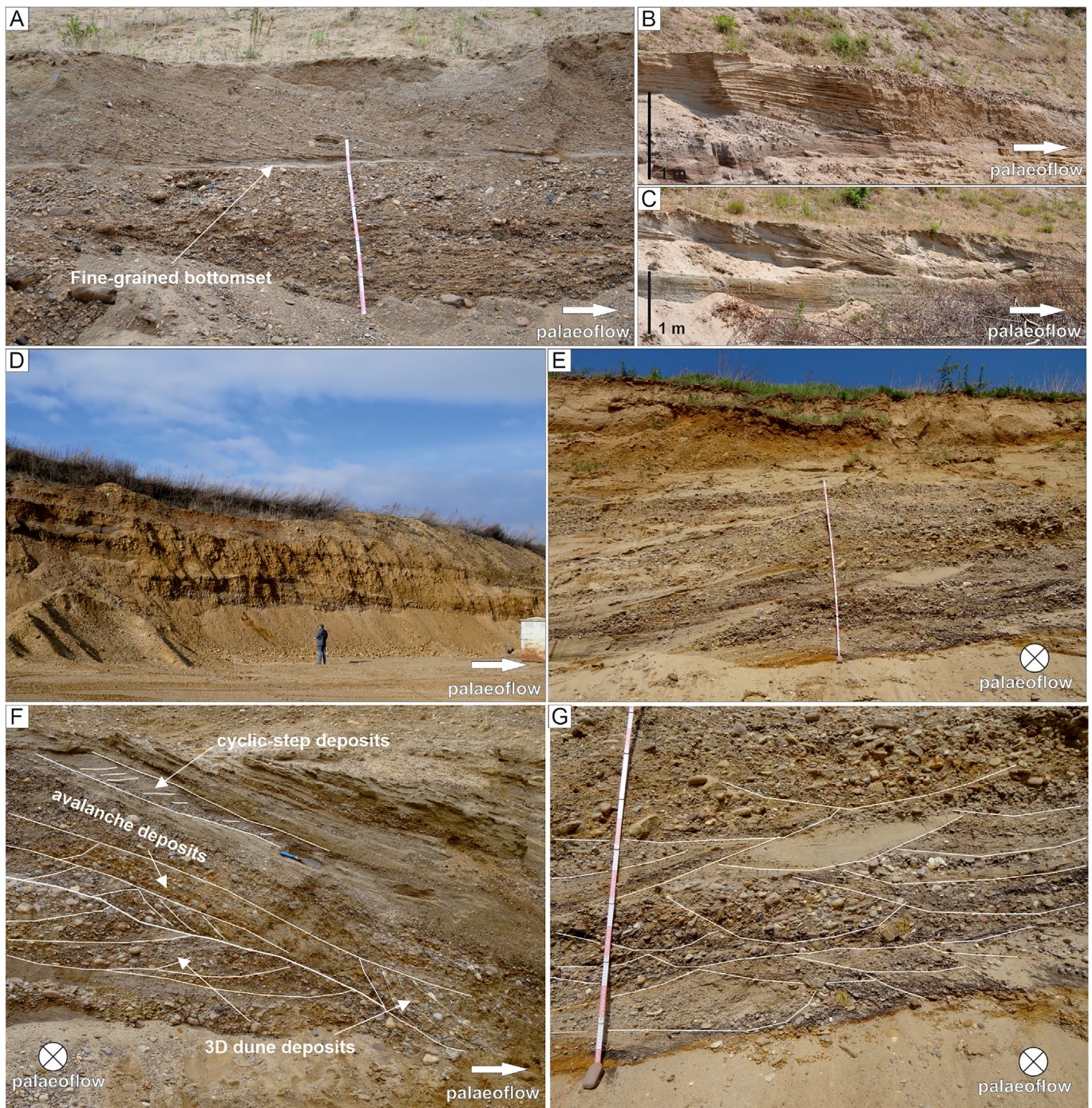
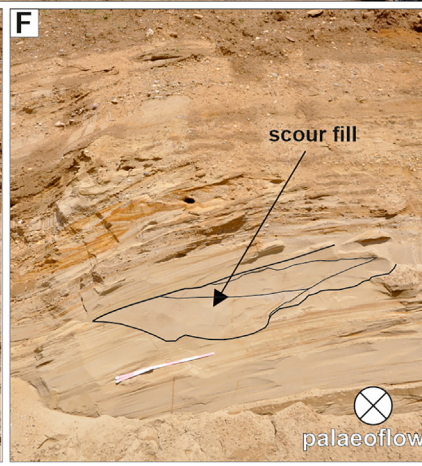
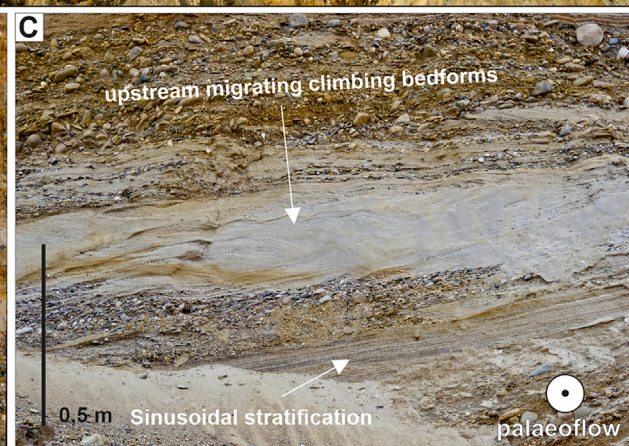
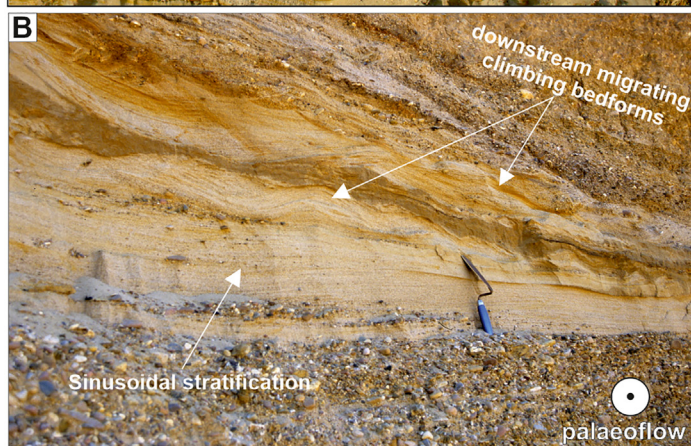
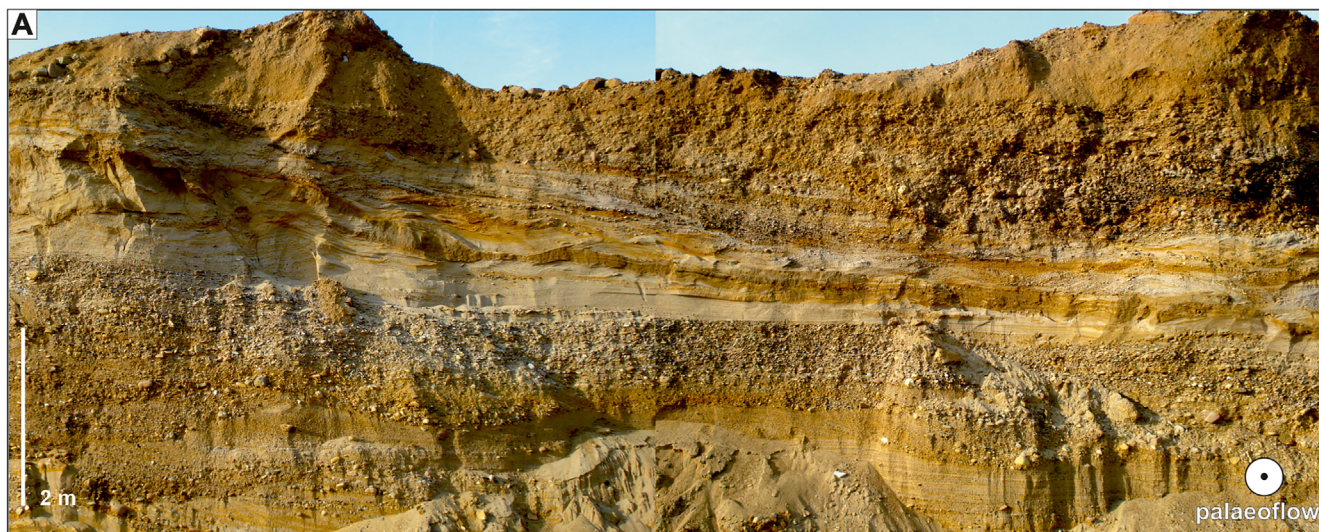


Fig. 4. Field examples of coarse-grained shallow-water mouth-bar systems, deposited from pure and stratified jets. A–C) Gravelly and sandy mouth-bars deposited from pure jets (Pleistocene Porta delta, Northern Germany). Foreset beds are deposited from avalanches and grain flows and commonly overlie thin fine-grained bottomsets. D–G) Gravelly mouth-bars deposited from stratified jets (Pleistocene Betheln delta, Northern Germany). D) Two vertically stacked proximal mouth bars, characterised by gravelly foresets deposited from grain avalanches and density flows that evolved on the lee side of the growing mouth bar. E) Close-up view of D) showing trough-cross-stratified foreset sediments. F) Close-up view of D) showing sandy backsets, overlying gravelly mouth-bar sediments deposited from grain avalanches and 3D dunes. The backsets indicate deposition from upslope migrating cyclic steps. Note different flow directions. Trowel for scale is 28 cm. G) Close-up view of E) showing trough-cross-stratified foreset sediments, interpreted to have been deposited by supercritical 3D dunes.

mouth bars record rapid cut-and-fill processes (Mutti et al., 2000; Ilgar and Nemeč, 2005; Rajchl et al., 2008; Fielding, 2010; Cole et al., 2021). Deformed beds, including load structures, slumps, ball-and-pillow structures and contorted bedding may also be common (e.g., Dunne and Hempton, 1984; Rajchl et al., 2008), implying rapid deposition with subsequent failure, slumping, liquefaction and soft sediment deformation.

3.2.2. Mouth bars dominated by tractional bedforms

Many sandy mouth bars are characterised by a distinct facies assemblage of coarse-grained planar, trough cross-stratified or low-angle cross-stratified sand(stones) passing downslope into finer-grained, massive or plane-parallel, “quasi” plane-parallel or subhorizontally stratified sand(stones) and eventually into climbing-ripple cross-laminated sand(stones) (Figs. 4E, F, G, 5, 6) reflecting deposition from



decelerating hyperpycnal turbulent and/or transitional flows. Beds have erosive, sharp or gradational basal contacts and are cm to dm thick (Mutti et al., 1996, 2000; Zavala et al., 2006; Olariu et al., 2010; Girard et al., 2012; Ahmed et al., 2014; Fidolini and Ghinassi, 2016; Zavala, 2020; Cole et al., 2021; Dou et al., 2021; Jin et al., 2021; Lin and Bhattacharya, 2021).

García-García et al. (2006), Ahmed et al. (2014), Martini and Sandrelli (2015), Fidolini and Ghinassi (2016), Ambrosetti et al. (2017), Van Yperen et al. (2020) and Melstrom and Birgenheier (2021) reported the occurrence of massive, normally or inversely graded sandstones and pebbly sandstones, alternating with trough cross-stratified and planar-parallel stratified sandstones, which may indicate the occurrence of avalanche and grain-flow processes on steeper mouth-bar slopes (Fig. 4F).

Massive sand(stones) or gravelly and sandy backsets filling spoon-shaped scours in the stoss and lee side deposits (Fig. 5F) are also common and record rapid cut-and-fill processes (Mutti et al., 2000; Ilgar and Nemeç, 2005; Rajchl et al., 2008; Fielding, 2010; Cole et al., 2021).

On closer inspection many of the described “massive, plane-parallel, quasi plane-parallel and subhorizontal stratification” show sinusoidal stratification that laterally pinches and swells due to slightly converging and diverging stratification and/or low-angle cross-sets dipping both upflow and downflow with common internal erosional truncations and small backsets, pointing to supercritical flow conditions and deposition by stable, migrating or breaking antidunes (Fig. 5A, B, C). Upslope climbing-ripple cross-lamination or backset cross-stratification (Figs. 4F, 5C) indicate deposition by cyclic steps (Allen, 1984; Alexander et al., 2001; Fielding, 2006, 2010; Girard et al., 2012; Lang and Winsemann, 2013; Cartigny et al., 2014; Lang et al., 2017b; Winsemann et al., 2018; Melstrom and Birgenheier, 2021; Ono et al., 2021; Tan and Plink-Björklund, 2021). Internally, beds may show a vertical cyclical recurrence of different sedimentary structures such as low-angle cross-stratification and (climbing-) ripple cross-lamination (Fig. 6A, C), indicating changing flow conditions under hyperpycnal flows (Zavala et al., 2006; Zavala, 2020), which may record the superposition of ripples onto larger antidunes in finer-grained sediments during generally supercritical flow conditions (cf., Fedele et al., 2016; for further discussion, see Section 4.2.2).

3.2.3. Large flute like erosional scours beneath mouth-bar deposits

Beneath mouth-bar deposits, large scours may occur. Erosional lower bounding surfaces are overlain by lag deposits of intraformational clasts and reworked fossils with a sandy matrix (e.g., Olariu and Bhattacharya, 2006; Zavala et al., 2006; Schomacker et al., 2010; Girard et al., 2012; Winsemann et al., 2018). Scours have also been described from modern depositional systems such as the Atchafalaya and Wax Lake Deltas (Roberts et al., 2003; Wellner et al., 2005), the Volga Delta (Overeem et al., 2003) and the Lena Delta (Are and Reimnitz, 2000). In flow direction, the lower bounding surface of mouth bars changes from being distinctly erosional in proximal parts to depositional towards the lateral and frontal margins of the bars. Schomacker et al. (2010) described large longitudinal scours from the Green River Formation, up to 8 m deep and approximately 300 m long. Perpendicular to the flow direction, the lower bounding surface is commonly concave-up in proximal positions, whereas depositional and nearly horizontal lower boundaries are more characteristic in distal

positions or in lateral positions towards mouth-bar margins (Schomacker et al., 2010).

The basal large scours and lag deposits of intraformational clasts, which underlie the mouth-bar deposits, indicate erosion and by-pass processes and are interpreted to have been incised by turbulent jet flows in front of the mouths of (terminal) distributary channels (e.g., Hoyal et al., 2003; Fielding et al., 2005; Olariu and Bhattacharya, 2006; Edmonds and Slingerland, 2007; Schomacker et al., 2010; Girard et al., 2012).

4. Discussion

4.1. Comparison of tank experiment and field examples

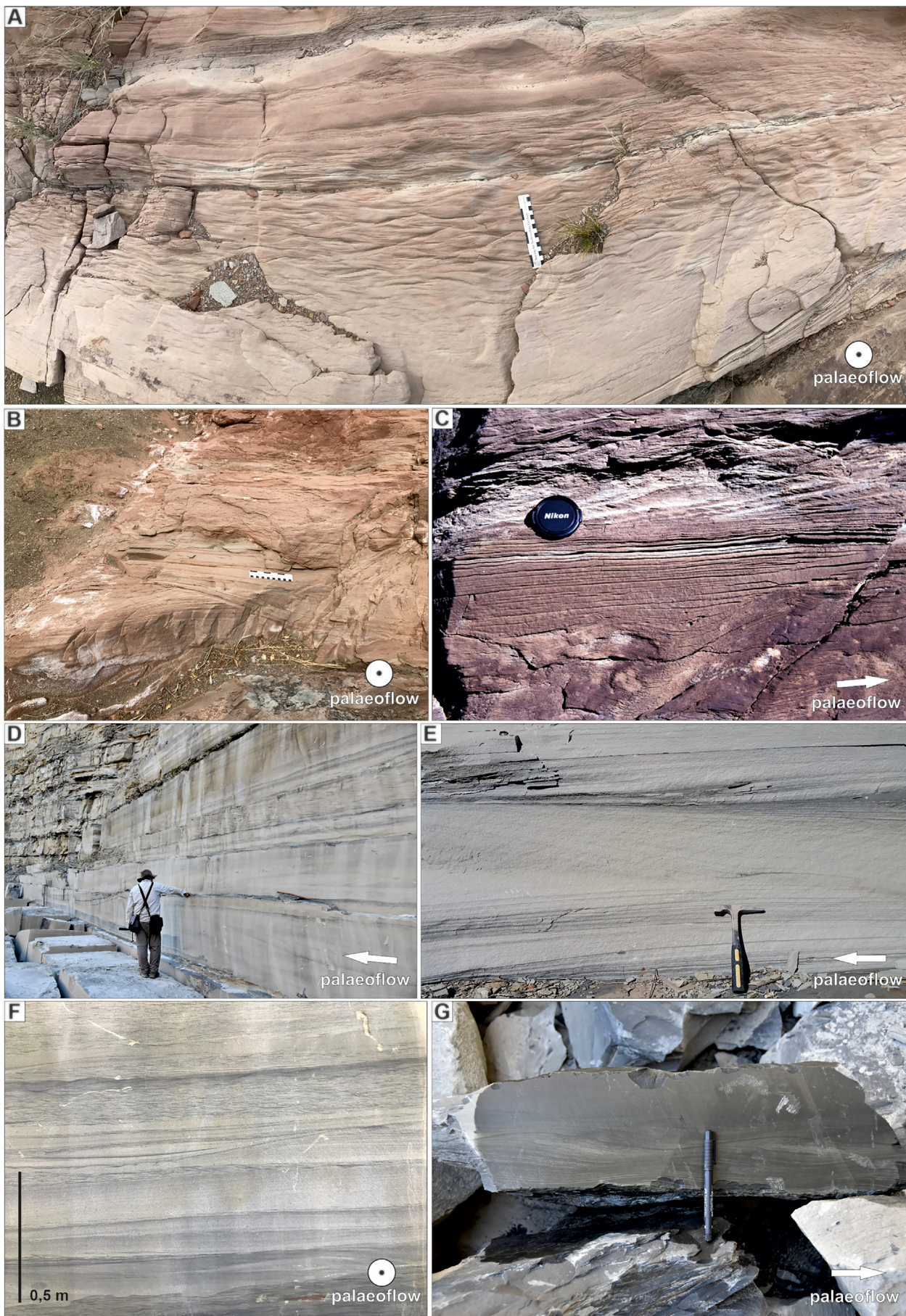
4.1.1. Geometry of scour-mouth-bar pairs

During all experiments when rapid mouth-bar growth took place, shallow scours formed in front of the orifice. These scours have length-width ratios between 1.18 and 2.21. The estimated length-width ratio of mouth bars varies between 1.54 and 2.36 with an overall radial or elongate pattern (Table 2). Scouring of the sediment bed and re-entrainment of the deposited sediment occurred in front of the orifice, where jets expanded by turbulent mixing with the ambient water at the flow interfaces. However, in all our experiments, deposition always exceeded erosion and the formation of a shallow bowl-shaped depression (scour) was restricted to the mouth-bar stoss side. Scour dimensions are controlled by the Froude number, initial flow density and sediment-bed grain size, with denser flows and finer-grained sediment leading to the formation of larger scours. Overall, the geometries and dimensions of the scour mouth-bar pairs were very similar to those formed in other jet experiments. Scours commonly widen and deepen with distance downstream to the region of maximum turbulence area where they shallow, widen and then merge with the depositional surface (e.g., Hoyal et al., 2003; Lang et al., 2021a). The area of erosion and bypass may be bounded by levees near the orifice (e.g., Van Wagoner et al., 2003; Daniller-Varghese et al., 2020).

However, the deep-water jets tended to produce deeper scours at the stoss side of the mouth bars than those of the shallow-water jets (Fig. 2H), corresponding with field observations in deep-water settings (e.g., Wynn et al., 2002; Winsemann et al., 2009; Macdonald et al., 2011; Hofstra et al., 2015; Brooks et al., 2018) and tank experiments (Lang et al., 2021a). This difference may be the result of more rapid sediment dumping due to more rapid flow deceleration and expansion in shallow water. More rapid sediment dumping is also responsible for the higher and steeper mouth bars formed by shallow-water jets compared with deep-water jets (Fig. 2H). Deceleration in shallow-water wall jets is rapid due to presence of both an upper (i.e., the water surface) and a lower (i.e., the bed) confinement to the flow, increasing the boundary friction (e.g., Wright, 1977; Launder and Rodi, 1983; Rowland et al., 2009; Fagherazzi et al., 2015). Compared with unbounded plane jets, lateral shear stresses and lateral diffusivity of momentum may be of an order of magnitude smaller close to the bottom than at the surface (Rowland et al., 2009).

The flute-like scours control the location of future (terminal) distributary channels (e.g., Van Wagoner et al., 2003; Martini and Sandrelli, 2015; Daniller-Varghese et al., 2020). They are infilled by aggradation, lateral or upstream migration of mouth bars (e.g., Van Wagoner et al., 2003; Olariu and Bhattacharya, 2006; Daniller-Varghese et al., 2020)

Fig. 5. Field examples of coarse-grained shallow-water mouth-bar systems, deposited from stratified jets (Pleistocene Betheln delta, Northern Germany). A) Mouth-bar sediments deposited from downstream and upstream migrating bedforms that developed beneath density flows. B) Close-up view of A) showing sandy intercalations of sinusoidal stratification and climbing-dune stratification, deposited from supercritical density flows that evolved on the lee side of the growing mouth bar. The sinusoidal stratification reflects deposition by stable antidunes, the short wavelength climbing dunes are interpreted as downstream migrating antidunes. Trowel for scale is 28 cm. C) Close-up view of A) showing short-wavelength upslope climbing sandy bedforms, interpreted as cyclic steps. D) Sandy mouth-bar sediments, deposited from migrating bedforms beneath density flows that developed on the lee side of the mouth bar. E) Close-up view of D) showing sinusoidal stratification, trough-cross stratification and climbing-ripple cross-lamination, deposited from super- and subcritical density flows. F) Close-up view of D) showing sinusoidally stratified sand, deposited from stationary antidunes, incised by a scour. The massive fill of the migrating scour reflects repeated cut-and-fill processes, probably related to breaking antidunes or the hydraulic-jump zone of cyclic steps. The scale is 60 cm.



or during periods of low discharge (Martini and Sandrelli, 2015; Daniller-Varghese et al., 2020). With time, the scour-mouth-bar pairs evolve into more complex sedimentary bodies (Van Wagoner et al., 2003; Edmonds and Slingerland, 2007; Daniller-Varghese et al., 2020). In response to continued mouth-bar aggradation, flow splitting occurs and smaller jets develop at the periphery of the mouth bar. Flow splitting will create knickpoints that migrate upflow, connect to the main channel and create a new incipient channel system that now captures most of the flow (cf., Van Wagoner et al., 2003). The experiments of Daniller-Varghese et al. (2020) show that channels stop bifurcating and begin migrating when the levee height reaches the same height as the mouth bar, and the channel incises into the mouth-bar deposits. If the channel deposits steepen to the degree that the mouth-bar deposits are at equal elevation, the channel erodes through it.

4.1.2. Deposition from sediment-laden pure (homopycnal) jets

The experiment with a sediment-laden pure jet implies that mouth-bar deposition and growth are dominated by avalanching on the front and, to a lesser amount, the sides of the mouth bar. Overpassing of the mouth bar by suspended load or saltation only occurred during the early flow stage as long as the mouth bar remained low. Mouth bars deposited by pure jets can thus be considered as avalanche- or grain-flow dominated systems with steep angle-of-repose foresets, prograding over subhorizontal bottomsets (Figs. 3A, D, 4A, B, C, 7A, B, D) (Wright, 1977; Dunne and Hempton, 1984; Mutti et al., 1996, 2000; Winsemann et al., 2009, 2018; Ahmed et al., 2014; Fidolini and Ghinassi, 2016; Ambrosetti et al., 2017; Cole et al., 2021).

Field examples show that these mouth-bar types may form laterally extensive bodies in flow direction (several tens to hundreds of metres) and display a typical three-partite topset-foreset-bottomset geometry. In transverse sections, these bars commonly form mounds, a few tens of metres wide and a few m thick. Internally mouth bars consist of convex-up, planar to sigmoidally cross-stratified gravel, pebbly sand, and sand, inclined at 5°–30° (e.g., Dunne and Hempton, 1984; Mutti et al., 1996, 2000; Rajchl et al., 2008; Winsemann et al., 2009, 2018; Ahmed et al., 2014; Fidolini and Ghinassi, 2016; Ambrosetti et al., 2017; Cole et al., 2021).

Clast-supported open-work gravel lenses and deformed beds indicate rapid deposition with subsequent slope failure, slumping, liquefaction and soft sediment deformation (e.g., Nemeč et al., 1999; Rajchl et al., 2008; Winsemann et al., 2018). Disconformities and reactivation surfaces are often overlain by thin sand or silt beds, pinching-out in a landward direction. These disconformities, reactivation surfaces, and thin beds of well-sorted sand and silt separating the coarser-grained foreset beds may reflect periods of reduced discharge and temporal inactivity of the mouth bars or lateral shifting and avulsion of the fluvial channel and depocentre, allowing for reworking of the mouth-bar deposits and deposition of thin sand beds by hyperpycnal flows (e.g., Sohn and Son, 2004; Ilgar and Nemeč, 2005; Zavala et al., 2006; Rajchl et al., 2008). Sand beds with upslope climbing-ripple cross-lamination (Fig. 5C) may represent deposits of small-scale cyclic steps (cf., Tan and Plink-Björklund, 2021) that formed under supercritical flow conditions during flood events.

Massive sandstones or gravelly and sandy backsets filling spoon-shaped scours in the stoss side deposits of mouth bars (e.g., Mutti et al., 2000; Cole et al., 2021) are related to the strong turbulence by the incoming jets, causing intense erosion and rapid backfilling of the scours. Massive sandstones or gravelly and sandy backsets filling spoon-shaped scours in the foreset toes may indicate hydraulic jumps (e.g., Rajchl et al., 2008), partly leading to the formation and local preservation of antidunes (e.g., Fielding, 2010). We did not observe hydraulic jumps in our experiments, but hydraulic jumps are likely to occur on the lower slope break, especially in settings with larger foreset heights (e.g., Nemeč et al., 1999; Winsemann et al., 2018; Tan and Plink-Björklund, 2021).

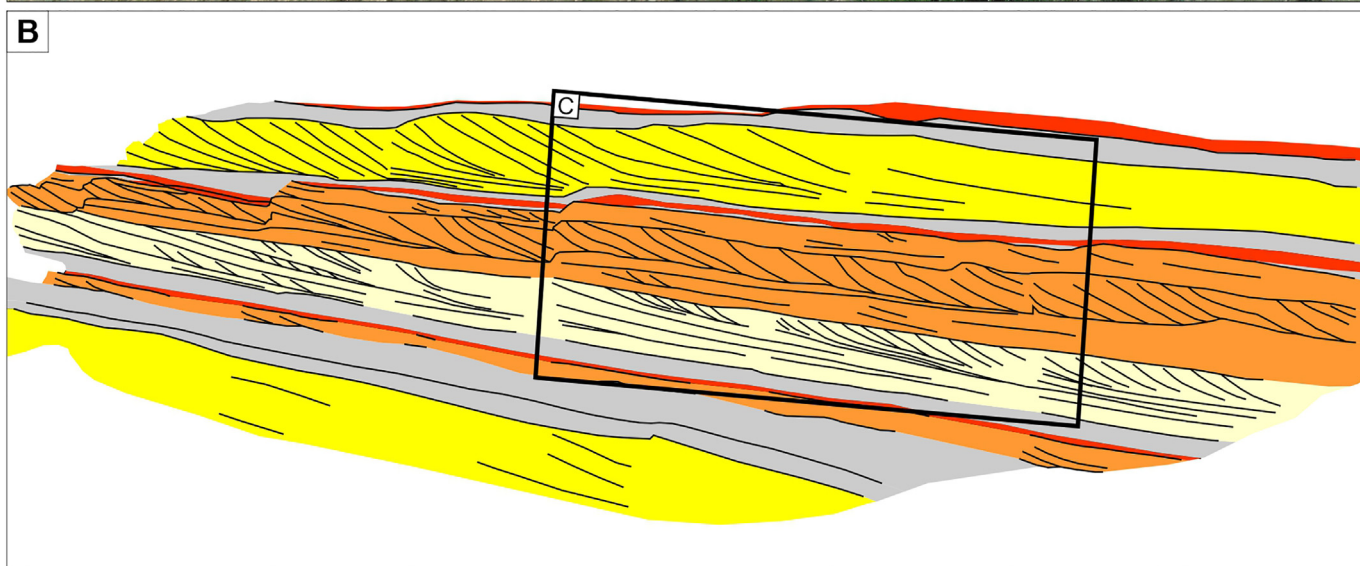
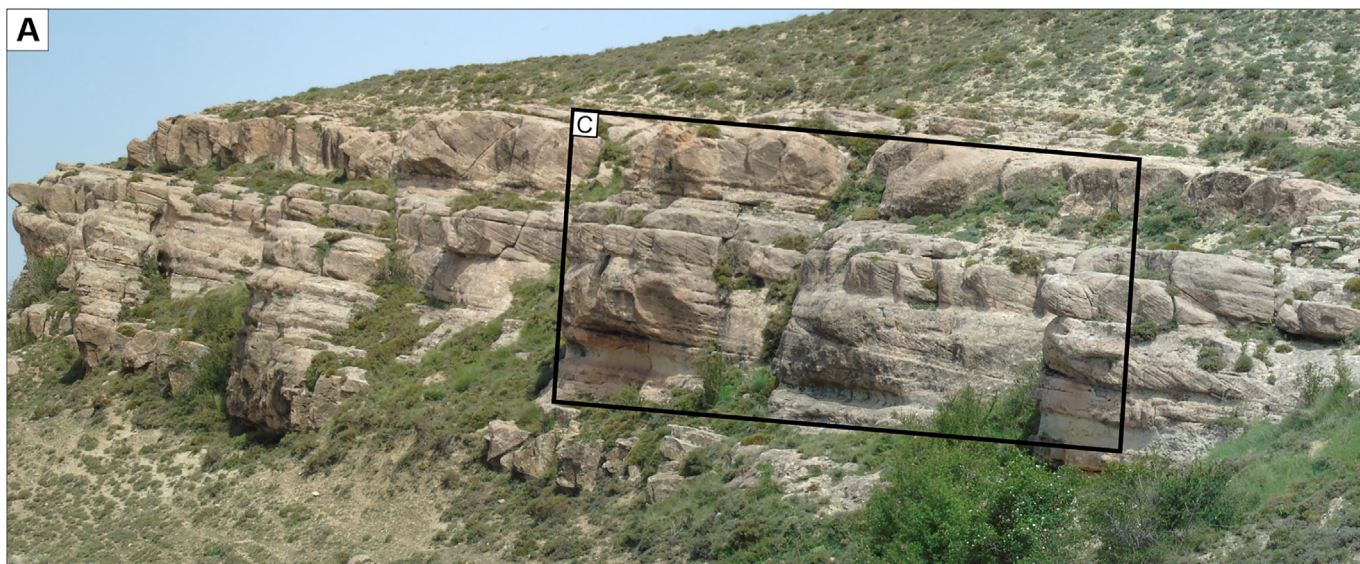
Sandy mouth-bar deposits commonly show less internal erosion surfaces and grain sizes vary from pebbly sand to very fine-grained sand. The coarser sandy beds are commonly massive, inversely or normally graded and may show pin-stripe stratification (Figs. 4B, C, 7D) (e.g., Mutti et al., 1996, 2000; Ilgar and Nemeč, 2005; Rajchl et al., 2008; Winsemann et al., 2009, 2018; Cole et al., 2021). Intercalated fine-grained beds may show (partly upslope) climbing-ripple cross-lamination (Ilgar and Nemeč, 2005; Rajchl et al., 2008), indicating deposition from (supercritical) hyperpycnal flows (cf., Tan and Plink-Björklund, 2021).

Mouth-bar overpassing may play a role in natural settings, where water depths are sufficient to maintain sediment transport (may be as ripples or dunes) on the mouth-bar top (e.g., Cole et al., 2021). For fluvial unit-bar deposits, Reesink and Bridge (2011) showed that the sorting, thickness and dip angle of the foresets are controlled by superimposed bedforms at the top of the unit-bar. The presence of superimposed bedforms results in the formation of thicker foreset laminae. Small superimposed bedforms affect the sorting pattern of the foresets due to pre-sorting in the superimposed bedforms, while large superimposed bedforms, attaining >25% of the bar height, will cause the formation of low-angle reactivation surfaces due to oblique-downflow migration of the superimposed bedforms. However, eventually channel bi-furcation or mouth-bar incision will occur and new bars will develop at the periphery (Van Wagoner et al., 2003; Olariu and Bhattacharya, 2006; Edmonds and Slingerland, 2007; Daniller-Varghese et al., 2020).




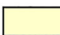

4.1.3. Deposition from stratified (hyperpycnal) jets

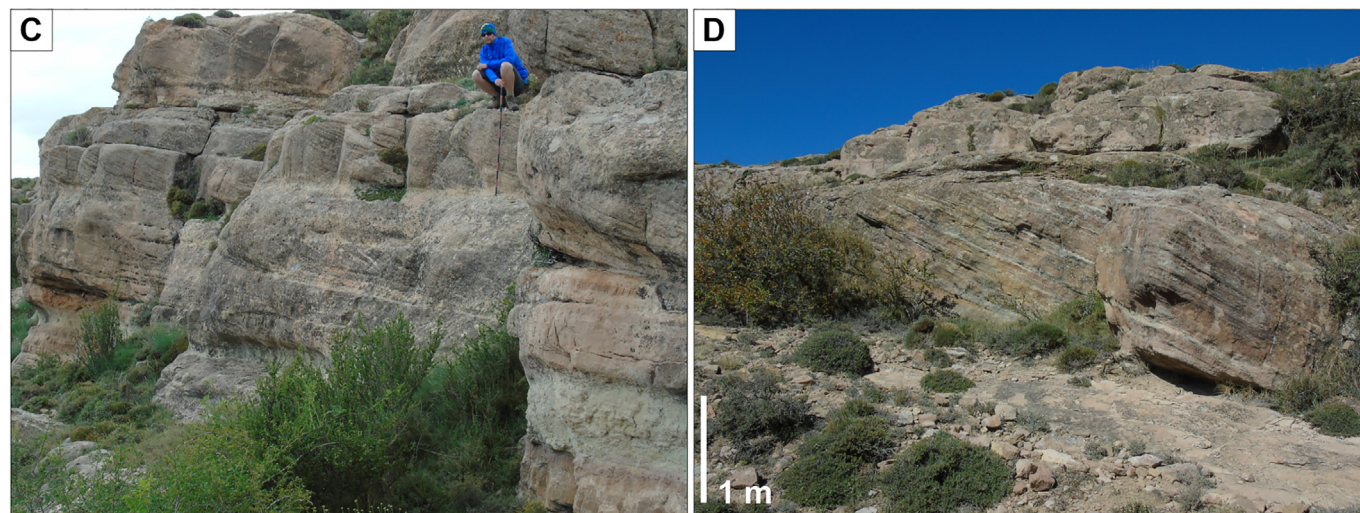
The experiments with sediment-laden stratified jets imply that mouth-bar deposition and growth are dominated by the density flows that evolved from the initial jets. The height of the mouth bar and the extent of the bedform field downslope of the mouth bars are controlled by the sediment-grain size. Beyond the mouth bar, flow processes and deposition are controlled by the characteristics of the density flow, which depend on excess density, grain size and basin slope. Mouth bars deposited by stratified jets can thus be considered as density flow-dominated. The observed asymmetrical downstream migrating bedforms on the lower lee side of the mouth bars and basinward of the mouth bars are interpreted as representing supercritical dunes and downstream migrating antidunes, as has been also observed in deep-water experiments by Fedele et al. (2016) and Lang et al.

Fig. 6. Field examples of fine-grained shallow-water delta lobes, deposited from density flows. A) Gradual vertical transition between low-angle cross-stratification and climbing-ripple cross lamination (Lower Cretaceous Rayoso Formation, Neuquen Basin, Argentina), probably indicating the superposition of ripples onto larger antidunes beneath Froude ($Fr > 1$) supercritical density flows. B) Fine-grained sandstones with HCS-like structures (Lower Cretaceous Rayoso Formation, Neuquen Basin, in Argentina). C) Gradual vertical transition between low-angle cross-stratification and climbing-ripple cross lamination (Lower Cretaceous Rayoso Formation, Neuquen Basin, Argentina; from Zavala et al., 2006 with permission), probably indicating the superposition of ripples onto larger antidunes beneath Froude ($Fr > 1$) supercritical density flows. D) Fine-grained low-angle cross-stratified and climbing-ripple cross-laminated delta front sandstones, deposited from supercritical and subcritical density flows (Upper Triassic Yanchang Formation, Ordos Basin, China). E) Close-up view of D) showing low-angle cross-stratified and sinusoidally stratified fine-grained sandstones, deposited from stable and breaking antidunes. Particulate organic matter is accumulated on bedding planes. F) Close-up view of D) showing alternations of low-angle cross-stratification, sinusoidal stratification and climbing-ripple cross-lamination. The sharp contacts between climbing-ripple cross-lamination and the larger-scale bedforms imply fluctuating supercritical and subcritical flows conditions (Upper Triassic Yanchang Formation, Ordos Basin, China). G) Very fine-grained delta-front sand- and siltstones with short wavelength climbing bedforms, probably reflecting downstream migrating antidunes (Upper Triassic Yanchang Formation, Ordos Basin, China). Pen for scale is 14 cm.



Key:

- | | | |
|---|--|---|
|  Granular lags (ravinement surfaces) |  Channel-fill deposits |  Coarse-grained mouth-bar deposits (deposited by grain avalanches) |
|  Sandy mouth-bar deposits (deposited by density flows) |  Prodelta deposits (massive bioturbated sandstones) | |



(2021a). As we could not measure the velocities during the tank experiments, we suggest by analogy to Fedele et al. (2016) and Lang et al. (2021a) that the proximal dunes are supercritical bedforms. In density flows, Froude supercritical flow conditions are reached at much lower velocities than in open-channel flows because of the reduced gravity (e.g., Fedele et al., 2016). Gravity forces acting on a submerged density flow need to be corrected for the density difference between the flow and the ambient water. The reduced gravity g' is given by $g' = g(\rho_f - \rho_w) / \rho_f$, where g is gravitational acceleration, ρ_f is the density of the flow and ρ_w is the density of the ambient water. The densimetric Froude number (Fr') is therefore given by $Fr' = \bar{u} / \sqrt{g' d}$, where \bar{u} is the mean flow velocity and d the flow depth. The reduced gravity will allow for Froude supercritical conditions (i.e., above unity) to be attained at lower flow velocities or larger flow depths. Furthermore, bedform stability fields differ strongly between (subaerial) open-channel flows and density flows due to differences in hydrodynamic and sediment-transport behaviour (Fedele et al., 2016; Koller et al., 2019; Lang et al., 2021a). Fedele et al. (2016) demonstrated that the stability field of ripples formed by density flows extends well into the Froude supercritical flow regime ($Fr' 1.1-1.3$). Downslope migrating asymmetrical dune-scale bedforms that formed under saline density flows generally require Froude supercritical flows ($Fr' > 1.5$) due to the high flow velocities needed to generate the necessary bed-shear stress. Dunes formed both under by-pass and aggrading conditions. Downstream migrating short antidunes (coarser grain sizes) and long upstream migrating antidunes (finer grain sizes) formed under lower Froude numbers ($Fr' < 1.5$). Plane-bed formation was not observed at densimetric Froude-critical flows. Upper-stage plane bed conditions were observed at densimetric Froude numbers > 2.2 , when antidunes became unstable due to increased flow competence and associated increased sediment resuspension from the bed. These plane-bed transitions were only observed for the finer sediment. For all other sediments, high densimetric Froude numbers produced cyclic steps from long antidunes (Fedele et al., 2016). At the antidune-plane bed transition, intense sediment entrainment into suspension dominated, and the proportion of suspension increased as antidunes flattened. Antidunes became slowly asymmetric downstream, rapidly decreasing in amplitude, and increasing in wavelength. Finer grained sediments favoured the formation and stability of long wavelength antidunes, probably caused by larger ratios of suspension-to-bed load. As grain size increased, bed-load transport became more dominant, probably favouring the growth of bed instabilities and formation of short downstream migrating antidunes and supercritical dunes (Fedele et al., 2016).

Many field studies show that mouth bars or delta-front lobes deposited from stratified jets (hyperpycnal flows) are characterised by a distinct facies assemblage (Figs. 4E, F, G, 5, 6, 7) of coarse-grained planar, trough cross-stratified or low-angle cross-stratified sand(stones) passing downslope into finer-grained, massive or subhorizontally stratified sand(stones) and eventually into climbing-ripple cross-laminated sand(stones). These facies transitions commonly occur over a short distance of a few tens to hundreds of metres (Martinsen, 1990; MacNaughton et al., 1997; Mutti et al., 2000, 2003; Olariu and Bhattacharya, 2006; Zavala et al., 2006; Fielding, 2010; Olariu et al., 2010; Schomacker et al., 2010; Girard et al., 2012; Ahmed et al., 2014; Martini and Sandrelli, 2015; Jerrett et al., 2016; Ambrosetti et al., 2017; Li et al., 2018; Van Yperen et al., 2020; Zavala, 2020; Cole et al., 2021; Melstrom and Birgenheier, 2021), implying deposition by decelerating (supercritical) flows. During initial mouth-bar growth, rapid aggradational deposition occurs from the decelerating, expanding jet, leading to the deposition of massive sand or pebbly sand with

bidirectional clinoforms, conformably offlapped by down-flow dipping clinoforms, characterised by tractional bedforms. Deep scouring and amalgamation related to the strong turbulence by the incoming jets are typical for the proximal upflow part, including massive gravel or sand or backsets filling spoon-shaped scours (e.g., Mutti et al., 2000, 2003; Cole et al., 2021).

García-García et al. (2006), Ahmed et al. (2014), Martini and Sandrelli (2015), Fidolini and Ghinassi (2016), Ambrosetti et al. (2017), Van Yperen et al. (2020) and Melstrom and Birgenheier (2021) reported the occurrence of massive, normally or inversely graded sandstones and pebbly sandstones, alternating with trough cross-stratified and planar-parallel stratified sandstones. The massive and graded deposits may either represent deposits of grain avalanches (grain flows) that evolved on the steep upper lee side of the coarse-grained mouth-bars, as observed in our experiments (run B, Figs. 2D, E, F, 3B, E) or surge-type turbidity currents that resulted from mouth bar failure and/or breaching (e.g., Van den Berg et al., 2002; Plink-Björklund and Steel, 2004; Olariu et al., 2010; Fidolini and Ghinassi, 2016). The vertical transition from conglomeratic beds into pebbly sandstone beds may reflect decreasing flow energies related to the growth of and decreasing depth over the mouth bar (cf., Edmonds and Slingerland, 2007; Van Yperen et al., 2020).

However, the scale up from metre-scale laboratory experiments to actual field examples remains a challenge and it must be considered that natural systems are much more complex than those of flume and tank models. The facies successions and the depositional architecture of shallow-water mouth bars may be far more complex than any experimental deposit. For instance, the grain-size distribution of the supplied sediment is commonly much wider, affecting the properties of the incoming jets, the evolving density flows and related bedforms (e.g., Ono et al., 2021). Fully turbulent density flows may evolve into transitional flows by incorporating mud and clay from the substrate, leading to the deposition of other (hybrid) bedform successions (e.g., Girard et al., 2012; Dou et al., 2021; Jin et al., 2021). A formal scaling between our experiments and natural systems was not sought in this study and experiments cannot be simply upscaled. However, the experiments should be considered as analogues to the natural systems, based on the similar flow, turbulence and transport regimes. It can be expected that sediment-transport and depositional processes (grain avalanches versus density flows) on the mouth bars observed in experimental flows, are similar to those occurring in nature. Upscaling is more problematic when comparing the dimension of mouth bars and bedforms. In nature, the dimensions of mouth bars will be several orders of magnitude larger than those of the bedforms. Therefore, it can be expected that the topography of bedforms, e.g., on the mouth-bar lee side, will have a much lower effect on sediment transport and the overall mouth-bar architecture than in the experiments. The same issue arises when comparing sediment-grain sizes to the outlet diameters or to the dimensions of the overall deposits.

4.2. Implications for the interpretation of lateral and vertical facies associations of shallow-water mouth bars/delta-front lobes

As outlined before, many of the described “massive, plane-parallel, quasi plane-parallel and subhorizontal stratification” show sinusoidal stratification that laterally pinches and swells due to slightly converging and diverging stratification and/or low-angle cross-sets dipping both upflow and downflow with common internal erosional truncations and small backsets, indicative of deposition by migrating, stable or breaking antidunes (e.g., Allen, 1984; Alexander et al., 2001; Russell

Fig. 7. Vertically stacked channel-mouth-bar complexes (marine Lower Cretaceous Xert formation, Maestrat basin, Spain). The view is oblique dip-oriented. Each channel-mouth-bar complex shows a shallowing-upward succession, separated by ravinement surfaces. All photographs by courtesy of G. Cole A) photo panel of vertically stacked channel-mouth-bar complexes. The mouth bars have been deposited from pure and stratified jets. B) Interpretation of photo panel (modified from Cole et al., 2018). C) Close-up view of A) showing cross-stratified, finer-grained mouth-bar sediments, deposited from downslope migrating dunes that evolved beneath stratified jets. Logging pole is 1.4 m long. D) Close-up view of A) showing steep, coarse-grained granular mouth-bar sediments, deposited from grain avalanches of pure jets.

and Arnott, 2003; Fielding, 2006, 2010; Duller et al., 2008; Girard et al., 2012; Lang and Winsemann, 2013; Cartigny et al., 2014; Fedele et al., 2016; Lang et al., 2017b; Winsemann et al., 2018; Melstrom and Birgenheier, 2021). Aggrading bedforms record a high sand-size suspension-load concentration that was maintained beyond the channel mouth (e.g., Girard et al., 2012; Lang and Winsemann, 2013; Lang et al., 2017b; Winsemann et al., 2018).

The formation of plane-parallel stratification, trough cross-stratification or low-angle cross-stratification was often attributed to lower flow regime “frictional flows”, whereas the formation of plane-parallel and climbing-ripple cross-lamination further downslope was attributed to inertial hyperpycnal flows. This downstream evolution has been attributed to shorter term variations in discharge, sediment flux and plume type, leading to deposits of hyperpycnal flows in the more distal lower part of detached mouth bars and delta front lobes during flood events and coarser-grained and steeper bedded sediments in the proximal upper part of the mouth bars by frictional flows during normal discharge conditions (Martinsen, 1990; Mutti et al., 1996, 2000; Zavala et al., 2006; Fielding, 2010; Ahmed et al., 2014; Jerrett et al., 2016). However, the results of flume and tank experiments (Fedele et al., 2016; Lang et al., 2021a, this study) imply that these observed downflow changes in bedforms may reflect deposition from

decelerating density flows that evolved on the lee slope of the mouth bar from supercritical stratified jets (Fig. 8B, C) and are not necessarily related to discharge, sediment flux and plume-type changes. The fine-grained load of these density flows is deposited on the lower mouth-bar slope and basinwards beyond the mouth bars. Subsequent progradation of the mouth bar will then lead to the observed increasingly coarser-grained and steeper bedded sediments.

Our tank experiments also imply that mouth bars deposited from stratified jets are less steep and less high than those deposited from pure jets, allowing for an effective sediment transport over the mouth bar and sediment transfer to delta lobes and the prodelta area by the density flow (Figs. 2, 3, 8; Supplementary data 1, 2).

A good field example for the grain-size control on mouth-bar heights is the Lower Cretaceous marine shallow-water delta of the Maestraz basin (NE Spain), where vertically stacked channel-mouth-bar complexes show an alternation of mouth bars deposited from pure and stratified jets (Fig. 7). The change from gently dipping, shallow mouth bars with tractive bedforms (3D dunes and ripples) towards higher and steeper mouth-bars deposited from grain flows has been attributed to the mouth-bar built up, avalanche (grain flow) slip face development and progradation into deeper water (Cole et al., 2021). However, this change instead may be related to a change in jet-flow properties in

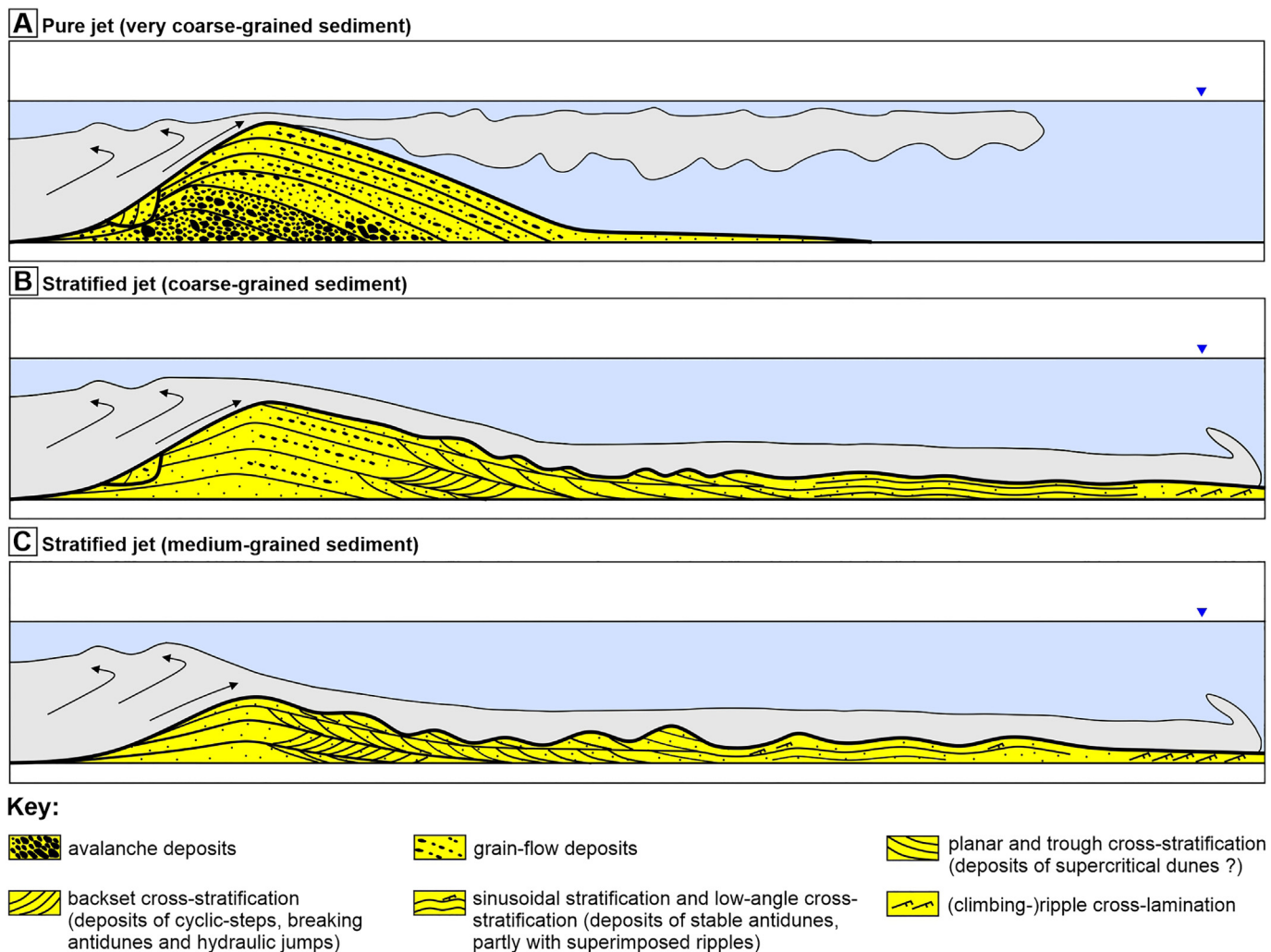


Fig. 8. Schematic sketches to illustrate the lateral facies associations of mouth-bars deposited from pure and stratified jets. Sketches are not to scale and are based on tank experiments and field examples. A) Depositional model for mouth bars deposited by pure jets with very coarse-grained sediment. Mouth bars are characterised by steep angle-of-repose cross bedding with related avalanche processes (grain flows) on the lee side. B) Depositional model for mouth bars deposited by stratified jets with coarse sediment. Deposition on the mouth-bar lee side is both from grain-flow avalanches and density flows. C) Depositional model for mouth bars deposited by stratified jets with medium-grained sediment. Mouth bars are characterised by a low relief. Deposition on the lee side is from density flows.

response to variations in water discharge/sediment supply. Seasonal or climatic-controlled variations in discharge and sediment supply will lead to a change in jet properties and the preferred evolution of either stratified or pure jets. During high discharge/flood conditions stratified jets will likely develop because of the increased grain transport in turbulent suspension at the river effluent (e.g., Mulder et al., 2003; Daniller-Varghese et al., 2020; Surlyk and Bruhn, 2020; Melstrom and Birgenheier, 2021), leading to the deposition of low, gently dipping mouth bars, characterised by tractive bedforms. Very coarse-grained stratified jets will evolve during exceptional flood events, such as glacial-lake outburst floods (e.g., Ghienne et al., 2010; Girard et al., 2012; Winsemann et al., 2018). The fully turbulent stratified jets may evolve into transitional flows by incorporating mud and clay from the substrate. Under transitional flows, mixed sand-mud bedforms may develop that are characterised by low-angle cross-stratification and large-scale ripple cross-lamination that may be mistaken for storm deposits (cf., Baas et al., 2016; Baker and Baas, 2020; Dou et al., 2021).

In contrast, during low discharge conditions pure jets will develop, because a higher amount of coarse sediment is transported as bed load, leading to the deposition of higher and steeper bedded mouth bars with angle-of-repose foresets (e.g., Martinsen, 1990; Mutti et al., 1996; Turner and Tester, 2006; Ahmed et al., 2014; Fagherazzi et al., 2015).

4.2.1. HCS- and SCS-like structures: wave-induced or formed by supercritical density flows?

HCS- and SCS-like structures have been frequently reported from marine and lacustrine shallow-water delta (mouth bar) deposits and are commonly attributed to wave-action or combined flows (Fig. 6B, C, F). These shallow-water deltas with HCS- and SCS-like structures may be characterised by distinct lateral and vertical facies successions with steep angle-of-repose cross-bedding in the proximal, up-flow part of mouth bars passing downflow and vertically into progressively finer-grained sandstones with SCS- or wavy HCS-like structures, “plane-parallel” stratification and ripple cross-lamination (MacNaughton et al., 1997; Mutti et al., 1996, 2000, 2003; Myrow et al., 2002; Zavala et al., 2006; Schomacker et al., 2010; Martini and Sandrelli, 2015; Lin and Bhattacharya, 2021). Steep-walled U- and shallower V-shaped gutter cast-like erosional features at the base of HCS-like structures and filled with massive, sinusoidally or low-angle cross-stratified sand were interpreted as subaqueous storm channels (e.g., Lin and Bhattacharya, 2021). However, it is noteworthy that these deposits with HCS- and SCS-like structures often lack wave-ripple cross-lamination at their tops as is typical for storm deposits. Myrow et al. (2002), Mutti et al. (2003), Zavala et al. (2006) and Martini and Sandrelli (2015) therefore already pointed out that not all these deposits may represent wave-induced structures but instead result from wave-modified density flows.

Studies on deposits of supercritical flows indicate that deposits of aggrading stable antidunes, breaking antidunes, chutes-and-pools and cyclic steps may strongly resemble HCS and SCS structures (Alexander et al., 2001; Fielding, 2006; Lang and Winsemann, 2013; Cartigny et al., 2014; Lang et al., 2017a, 2017b, 2021b; Massari, 2017; Vaucher et al., 2018; Slooman and Cartigny, 2020; Ono et al., 2021; Postma et al., 2021; Slooman et al., 2021). The pinch-and-swell geometry of aggrading stable antidune deposits resembles isotropic HCS structures whereas the low-angle cross-stratification of migrating antidunes may resemble anisotropic HCS structures, which therefore can be misinterpreted as wave-induced structures. Deposits of chutes-and-pools can be mistaken for wave-induced SCS structures. Chutes-and-pools are unstable supercritical bedforms that are characterised by lenticular scours infilled by backset cross-stratified sand and pebbly sand or gravels. Backsets have concave-up, downflow divergent geometries and may display downflow transitions to convex-up or sigmoidal geometries (Lang and Winsemann, 2013; Cartigny et al., 2014; Lang et al., 2017b; Postma et al., 2021; Slooman et al., 2021).

According to our tank experiments the lateral and vertical facies successions with steep angle-of-repose cross-bedding passing downflow and vertically into progressively finer-grained deposits with SCS- and HCS-like structures, “plane-parallel” stratification and ripple cross-lamination, more likely indicate deposition from sediment-laden stratified jets. Initial deposition occurred from grain avalanches on the lee slope of the growing mouth bar, followed by tractional deposition of decelerating supercritical density flows that evolved on the steepening lee side of the mouth bar. Steep-walled U- and shallower V-shaped erosional features, filled with massive, sinusoidally or low-angle cross-stratified sandstones may instead represent rapid cut-and-fill processes in the hydraulic jump zone of breaking antidunes, chutes-and-pools or cyclic steps (Fielding, 2010; Lang and Winsemann, 2013; Lang et al., 2017a, 2017b; Winsemann et al., 2018; Postma et al., 2021; Slooman et al., 2021).

4.2.2. Ripple formation under supercritical density flows?

Myrow et al. (2002), Zavala et al. (2006), Olariu et al. (2010) and Van Yperen et al. (2020) observed repeated vertical transitions between climbing-ripple cross-lamination and low-angle cross-stratification, partly interpreted as deposits of combined flows (e.g., Myrow et al., 2002). This cyclical recurrence of low-angle cross-stratified and climbing-ripple cross-laminated sand(stone) (Fig. 6A, C) instead may indicate the superposition of ripples onto larger antidunes in finer-grained sediments. In the flume experiments of Fedele et al. (2016), ripples superposed onto larger, upstream migrating antidunes in finer-grained sediments for a range of the densimetric Froude numbers of 1.1 to 1.3. In these experiments, ripples formed beneath subcritical, critical and slightly supercritical density flows, in contrast to open-channel flows, where ripples exclusively form in the lower flow regime (see also Hand, 1974). When the densimetric Froude numbers increased beyond 1.3, ripples became unstable as entrainment of bed sediment into the suspension increased and the larger, upstream migrating antidunes became the only stable bedforms (Fedele et al., 2016). These bedform successions may therefore indicate changing flow conditions under thin hyperpycnal flows (Fedele et al., 2016), which in turn may be related to the evolving bed morphology and the spatio-temporal evolution of the formative flow (Zavala et al., 2006; Lang et al., 2017a). If boundaries between these beds with climbing-ripple cross-lamination and low-angle cross-stratification are sharp, the vertical succession may record variation of discharge during flood events and interflow periods (e.g., Mulder et al., 2003; Olariu et al., 2010; Van Yperen et al., 2020).

5. Conclusions

Our experiments with pure and stratified jets imply that the heights, geometries and bedforms / sedimentary structures of mouth bars depend on jet properties and grain size of the supplied sediment. Shallow flute-like scours formed in front of the orifice. Scour dimensions are controlled by the initial flow density and sediment-bed grain size, with denser flows and finer-grained sediment leading to the formation of larger scours. However, deposition always exceeded erosion and the formation of a shallow bowl-shaped depression (scour) was restricted to the mouth-bar stoss side.

Initial mouth-bar growth occurred from vertical aggradation with a bi-directional dip of the depositional surface and was followed by lateral expansion and vertical accretion. Rapid deposition probably resulted from deceleration of shallow-water wall jets due to presence of both an upper and a lower flow confinement, increasing the boundary friction. The stoss sides of mouth bars were affected by intense turbulence of the incoming jets, causing scouring and constant remobilisation of sediment.

In pure jets with very coarse-grained sediment a high and steep mouth bar formed, characterised by steep angle-of-repose cross bedding with related avalanche processes (grain flows) on the lee side. In experiments with stratified jets, mouth-bar deposition and growth

was dominated by supercritical density flows that evolved from the initial jets on the lee side of the growing mouth bar. After initial mouth-bar growth by the dumping of bed load in front of the orifice, a density flow formed on the lee side of the mouth bar. The density flow caused the formation of bedforms on the slope of the mouth bar and on the sediment bed further downslope. The height of the mouth bars and the extent of the bedform field downslope of the mouth bars were controlled by the sediment-grain size. Beyond the mouth bar, flow processes and deposition were controlled by the characteristics of the density flow, which depend on the excess of density, grain size and bed slope. In stratified jets with very coarse-grained sediment, deposition on the mouth-bar lee side was both from grain flows and density flows. Deposition on the upper lee slope was dominated by grain flows. On the lower slope and in fine-grained bed material beyond the mouth bar, a concentric field of low relief, asymmetric, downflow-migrating bedforms evolved. In stratified jets with medium-grained sediment a very low mouth bar formed with a concentric field of low relief, asymmetric, downflow-migrating bedforms covering the entire lee slope. The observed asymmetrical downstream migrating bedforms on the lower lee side of the mouth bars and basinward of the mouth bars are interpreted as representing supercritical dunes and downstream migrating antidunes because in density flows, supercritical flow conditions are reached at much lower velocities than in open-channel flows because of the reduced gravity.

The review of field-based studies implies that a wider range of sedimentary structures may occur in mouth bars in comparison to our experiments. However, natural systems are much more complex than those of flume and tank models and a simple upscaling by a single similarity law is not possible. Lateral facies assemblages of coarse-grained cross-stratified or low-angle cross-stratified sand(stones) passing downslope into finer-grained HCS-like structures, “quasi-parallel” laminated sand, and into climbing-ripple cross-laminated sand(stones) are commonly reported from field examples. However, on closer inspection many of the described “quasi-parallel” structures show sinusoidal stratification that laterally pinches and swells due to slightly converging and diverging stratification and/or low-angle cross-sets dipping both upflow and downflow with common internal erosional truncations and small backsets, indicative of deposition by migrating, stable or breaking antidunes. Comparison with flume and tank experiments suggests that the proximal coarse-grained planar and trough cross-stratified sandstones represent deposits of supercritical dunes that pass downslope into antidune deposits, characterised by sinusoidal stratification and/or low-angle cross stratification. Repeated vertical transitions between antidune deposits and climbing-ripple cross-laminated sand(stone) may indicate the superposition of ripples onto antidunes in finer-grained sediments and ripple formation under supercritical flow conditions. Similar bedforms have previously been interpreted as HCS- or SCS-like structures and attributed to combined flows in storm-dominated settings, which probably in some cases has to be revised.

Supplementary data to this article can be found online at <https://doi.org/10.1016/j.sedgeo.2021.105962>.

Declaration of competing interest

The authors declare that they have no known competing financial interests or personal relationships that could have appeared to influence the work reported in this paper.

Acknowledgement

We thank Travis Swanson, an anonymous reviewer and editor Catherine Chagué for constructive comments, which helped to improve the manuscript. We are grateful for the support by ExxonMobil Upstream Research Company for providing access to the experimental facility and supplying the consumables for the experiments. We thank T. Bover

Arnal, C. Brandes, G. Cole, R. Jerrett, M. Ghinassi, M. Rajchl, P.P. Rodriguez Lopez, Y. Spychala, R. Tinterri, D. Uličný and M. Watkinson for discussion, providing photographs and regional literature. Tim Hartmann and Jan Redeker helped with artwork. Special thanks go to the landowners, who granted access to open-pits and outcrops. Partial funding of the research work by the German Research Foundation (DFG; Grant LA 4422/1-1) is greatly appreciated.

References

- Ade, F., Rajaratnam, N., 1998. Generalized study of erosion by circular horizontal turbulent jets. *Journal of Hydraulic Research* 36, 613–636.
- Ahmed, S., Bhattacharya, J.P., Garza, D.E., Li, Y., 2014. Facies architecture and stratigraphic evolution of a river-dominated delta front, Turonian Ferron Sandstone, Utah, USA. *Journal of Sedimentary Research* 84, 97–121.
- Alexander, J., Bridge, J.S., Cheel, R.J., Leclair, S.F., 2001. Bedforms and associated sedimentary structures formed under supercritical water flows over aggrading sand beds. *Sedimentology* 48, 133–152.
- Allen, J.R.L., 1984. Sedimentary structures: their character and physical basis. *Developments in Sedimentology* 30, 1–663.
- Ambrosetti, E., Martini, I., Sandrelli, F., 2017. Shoal-water deltas in high-accommodation settings: insights from the lacustrine Valimi Formation (Gulf of Corinth, Greece). *Sedimentology* 64, 425–452.
- Are, F., Reimnitz, E., 2000. An overview of the Lena River Delta setting: geology, tectonics, geomorphology, and hydrology. *Journal of Coastal Research* 16, 1083–1093.
- Baas, J.H., Best, J.L., Peakall, J., 2016. Predicting bedforms and primary current stratification in cohesive mixtures of mud and sand. *Journal of the Geological Society* 173, 12–45.
- Baker, M.L., Baas, J.H., 2020. Mixed sand-mud bedforms produced by transient turbulent flows in the fringe of submarine fans: indicators of flow transformation. *Sedimentology* 67, 2645–2671.
- Bates, C.C., 1953. Rational theory of delta formation. *AAPG Bulletin* 37, 2119–2162.
- Brooks, H.L., Hodgson, D.M., Brunt, R.L., Peakall, J., Hofstra, M., Flint, S.S., 2018. Deep-water channel-lobe transition zone dynamics: processes and depositional architecture, an example from the Karoo Basin, South Africa. *American Society of Geologists Bulletin* 130, 1723–1746.
- Cao, Y., Wang, Y., Gluyas, J.G., Liu, H., Liu, H., Song, M., 2018. Depositional model for lacustrine nearshore subaqueous fans in a rift basin: the Eocene Shahejie Formation, Dongying Sag, Bohai Bay Basin, China. *Sedimentology* 65, 2117–2148.
- Cartigny, M.J.B., Ventra, D., Postma, G., Van den Berg, J.H., 2014. Morphodynamics and sedimentary structures of bedforms under supercritical-flow conditions: new insights from flume experiments. *Sedimentology* 61, 712–748.
- Chough, S.K., Hwang, I.G., 1997. The Duksung fan delta, SE Korea: growth of delta lobes on a Gilbert-type topset in response to relative sea-level rise. *Journal of Sedimentary Research* 67, 725–739.
- Chu, V.H., Baddour, R.E., 1984. Turbulent gravity-stratified shear flows. *Journal of Fluid Mechanics* 138, 353–378.
- Cole, G., Watkinson, M.P., Jerrett, R., Anderson, I., 2018. Architectural Analysis of Tectonically Influenced Shallow Water Mouth Bar Complexes, Lower Cretaceous Maestrat Basin, Spain: Implications for Reservoir Characterization and Modelling (http://www.searchanddiscovery.com/documents/2018/11042cole/cole_presentation.pdf. (AAPG/Datapages, Inc., 1444 South Boulder, Tulsa, OK, 74119, USA)).
- Cole, G., Jerrett, R., Watkinson, M.P., 2021. A stratigraphic example of the architecture and evolution of shallow water mouth bars. *Sedimentology* 68, 1227–1254.
- Daniller-Varghese, M.S., Kim, W., Mohrig, D.C., 2020. The effect of flood intermittency on bifurcations in fluviodeltaic systems: experiment and theory. *Sedimentology* 67, 3055–3066.
- Dietrich, P., Ghienne, J.-F., Normandeau, A., Lajeunesse, P., 2016. Upslope-migrating bedforms in a proglacial sandur delta: cyclic steps from river-derived underflows? *Journal of Sedimentary Research* 86, 113–123.
- Dou, L., Best, J., Bao, Z., Hou, J., Zhang, L., Liu, Y., 2021. The sedimentary architecture of hyperpycnites produced by transient turbulent flows in a shallow lacustrine environment. *Sedimentary Geology* 411, 105804. <https://doi.org/10.1016/j.sedgeo.2020.105804>.
- Dowdeswell, J.A., Hogan, K.A., Arnold, N.S., Mugford, R.I., Wells, M., Hirst, J.P.P., Decalf, C., 2015. Sediment-rich meltwater plumes and ice-proximal fans at the margins of modern and ancient tidewater glaciers: observations and modelling. *Sedimentology* 62, 1665–1692.
- Duller, R.A., Mountney, N.P., Russell, A.J., Cassidy, N.C., 2008. Architectural analysis of a volcanoclastic jökulhlaup deposit, southern Iceland: sedimentary evidence for supercritical flow. *Sedimentology* 55, 939–964.
- Dunne, L.A., Hempton, M.R., 1984. Deltaic sedimentation in the Lake Hazar pull-apart basin, south-eastern Turkey. *Sedimentology* 31, 401–412.
- Edmonds, D.A., Slingerland, R.L., 2007. Mechanics of river mouth bar formation: implications for the morphodynamics of delta distributary networks. *Journal of Geophysical Research* 112, F02034. <https://doi.org/10.1029/2006JF005074>.
- Ellison, T.H., Turner, J.S., 1959. Turbulent entrainment in stratified flows. *Journal of Fluid Mechanics* 6, 423–448.
- Eriksson, P.G., Condie, K.C., Tirsgaard, H., Mueller, W.U., Altermann, W., Miall, A.D., Aspler, L.B., Cataneanu, O., Chiarenzelli, J.R., 1998. Precambrian clastic sedimentation systems. *Sedimentary Geology* 120, 5–53.
- Fagherazzi, S., Edmonds, D.A., Nardin, W., Leonardi, N., Canestrelli, A., Falcini, F., Jerolmack, D.J., Mariotti, G., Rowland, J.C., Slingerland, R.L., 2015. Dynamics of river mouth deposits. *Reviews of Geophysics* 53, 642–672.

- Fedele, J.J., Hoyal, D.C., Bamaal, Z., Tulenko, J., Awalt, S., 2016. Bedforms created by gravity flows. In: Budd, D., Hajek, E., Purkis, S. (Eds.), *Autogenic Dynamics and Self-organization in Sedimentary Systems*. 106. SEPM, Special Publications, pp. 95–121.
- Fidolini, F., Ghinassi, M., 2016. Friction-and inertia-dominated effluents in a lacustrine, river-dominated deltaic succession (Pliocene upper Valdarno Basin, Italy). *Journal of Sedimentary Research* 86, 1083–1101.
- Fielding, C.R., 2006. Upper flow regime sheets, lenses and scour fills: extending the range of architectural elements for fluvial sediment bodies. *Sedimentary Geology* 190, 227–240.
- Fielding, C.R., 2010. Planform and facies variability in asymmetric deltas: facies analysis and depositional architecture of the Turonian Ferron Sandstone in the western Henry Mountains, south-central Utah, USA. *Journal of Sedimentary Research* 80, 455–479.
- Fielding, C.R., Trueman, J.D., Alexander, J., 2005. Sharp-based, flood-dominated mouth bar sands from the Burdekin River Delta of northeastern Australia: extending the spectrum of mouth-bar facies, geometry, and stacking patterns. *Journal of Sedimentary Research* 75, 55–66.
- Fischer, H.B., List, J.E., Koh, C.R., Imberger, J., Brooks, N.H., 1979. *Mixing in Inland and Coastal Waters*. Academic Press, New York (483 pp).
- García-García, F., Fernández, J., Viseras, C., Soria, J.M., 2006. Architecture and sedimentary facies evolution in a delta stack controlled by fault growth (Betic Cordillera, southern Spain, late Tortonian). *Sedimentary Geology* 185, 79–92.
- Ghienne, J.-F., Girard, F., Moreau, J., Rubino, J.-L., 2010. Late Ordovician climbing dune assemblages: a signature of outburst flood in proglacial outwash environments? *Sedimentology* 57, 1175–1198.
- Ghinassi, M., 2007. The effects of differential subsidence and coastal topography on high-order transgressive-regressive cycles: Pliocene nearshore deposits of the Val d'Orcia Basin, Northern Apennines, Italy. *Sedimentary Geology* 202, 677–701.
- Girard, F., Ghienne, J.F., Rubino, J., 2012. Occurrence of hyperpycnal flows and hybrid event beds related to glacial outburst events in a Late Ordovician proglacial delta (Murzuk Basin, SW Libya). *Journal of Sedimentary Research* 82, 688–708.
- Gobo, K., Ghinassi, M., Nemeč, W., 2014. Reciprocal changes in foreset to bottomset facies in a Gilbert-type delta: response to short-term changes in base level. *Journal of Sedimentary Research* 84, 1079–1095.
- Hage, S., Cartigny, M.J., Sumner, E.J., Clare, M.A., Hughes Clarke, J.E., Talling, P.J., Lintern, D.G., Simmons, S.M., Silva Jacinto, R., Vellinga, A.J., Allin, J.R., 2019. Direct monitoring reveals initiation of turbidity currents from extremely dilute river plumes. *Geophysical Research Letters* 46, 11310–11320.
- Hamilton, P.B., Strom, K.B., Hoyal, D.C., 2015. Hydraulic and sediment transport properties of autogenic avulsion cycles on submarine fans with supercritical distributaries. *Journal of Geophysical Research - Earth Surface* 120, 1369–1389.
- Hamilton, P., Gaillot, G., Strom, K., Fedele, J., Hoyal, D., 2017. Linking hydraulic properties in supercritical submarine distributary channels to depositional-lobe geometry. *Journal of Sedimentary Research* 87, 935–950.
- Hand, B.M., 1974. Supercritical flow in density currents. *Journal of Sedimentary Petrology* 44, 637–648.
- Hofstra, M., Hodgson, D.M., Peakall, J., Flint, S.S., 2015. Giant scour-fills in ancient channel-lobe transition zones: formative processes and depositional architecture. *Sedimentary Geology* 329, 98–114.
- Hoyal, D.C.J.D., Van Wagoner, J.C., Adair, N.L., Deffenbaugh, M., Li, D., Sun, T., Huh, C., Griffin, D.E., 2003. Sedimentation from jets: a depositional model for clastic deposits of all scales and environments. *Search and Discovery*, 40082.
- Hughes Clarke, J.E., 2016. First wide-angle view of channelized turbidity currents links migrating cyclic steps to flow characteristics. *Nature Communications* 7, 118960. <https://doi.org/10.1038/ncomms11896>.
- Hwang, I.G., Chough, S.K., Hong, S.W., Choe, M.Y., 1995. Controls and evolution of fan delta systems in the Miocene Pohang Basin, SE Korea. *Sedimentary Geology* 98, 147–179.
- Ilgar, A., Nemeč, W., 2005. Early Miocene lacustrine deposits and sequence stratigraphy of the Ermenk Basin, Central Taurides, Turkey. *Sedimentary Geology* 173, 233–275.
- Jerrett, R.M., Bennie, L.L., Flint, S.S., Greb, S.F., 2016. Extrinsic and intrinsic controls on mouth bar and mouth bar complex architecture: examples from the Pennsylvanian (Upper Carboniferous) of the central Appalachian Basin, Kentucky, USA. *Geological Society of America Bulletin* 128, 1696–1716.
- Jin, L., Shan, X., Shi, X., Fonesu, M., Qiao, S., Kandasamy, S., Wang, H., Liu, S., Fang, X., Zou, X., 2021. Hybrid event beds generated by erosional bulking of modern hyperpycnal flows on the Choshui River delta front, Taiwan Strait. *Sedimentology* <https://doi.org/10.1111/sed.12862>.
- Jirka, G.H., 2004. Integral model for turbulent buoyant jets in unbounded stratified flows. Part I: single round jet. *Environmental Fluid Mechanics* 4, 1–56.
- Koller, D., Manica, R., Oliveira Borges, A., Fedele, J.J., 2019. Experimental bedforms by saline density currents. *Brazilian Journal of Geology* 49, e20180118. <https://doi.org/10.1590/2317-4889201920180118>.
- Kurcinka, C., Dalrymple, R.W., Gugliotta, M., 2018. Facies and architecture of river-dominated to tide-influenced mouth bars in the lower Lajas Formation (Jurassic), Argentina. *AAPG Bulletin* 102, 885–912.
- Lang, J., Winsemann, J., 2013. Lateral and vertical facies relationships of bedforms deposited by aggrading supercritical flows: from cyclic steps to humpback dunes. *Sedimentary Geology* 296, 36–54.
- Lang, J., Dixon, R.J., Le Heron, D.P., Winsemann, J., 2012. Depositional architecture and sequence stratigraphic correlation of Upper Ordovician glacial deposits, Illizi Basin, Algeria. In: Huuse, M., Redfern, J., Le Heron, D.P., Dixon, R.J., Moscardello, A., Craig, J. (Eds.), *Glaciogenic Reservoirs and Hydrocarbon Systems*. Geological Society, London, Special Publications 368, pp. 293–317.
- Lang, J., Brandes, C., Winsemann, J., 2017a. Erosion and deposition by supercritical density flows during channel avulsion and backfilling: Field examples from coarse-grained deepwater channel-levée complexes (Sandino Forearc Basin, southern Central America). *Sedimentary Geology* 349, 79–102.
- Lang, J., Sievers, J., Loewer, M., Igel, J., Winsemann, J., 2017b. 3D architecture of cyclic step and antidune deposits in glaciogenic subaqueous fan and delta settings: integrating outcrop and ground-penetrating radar data. *Sedimentary Geology* 362, 83–100.
- Lang, J., Fedele, J.J., Hoyal, D.C.J.D., 2021a. Three-dimensional submerged wall jets and their transition to density flows – morphodynamics and implications for the depositional record. *Sedimentology* 68, 1297–1327.
- Lang, J., Le Heron, D.P., Van den Berg, J.H., Winsemann, J., 2021b. Bedforms and sedimentary structures related to supercritical flows in glaciogenic settings. *Sedimentology* 68, 1539–1579.
- Lauder, B.E., Rodi, W., 1983. The turbulent wall jet measurements and modeling. *Annual Review of Fluid Mechanics* 15, 429–459.
- Leren, B.L., Howell, J., Enge, H., Martinus, A.W., 2010. Controls on stratigraphic architecture in contemporaneous delta systems from the Eocene Roda Sandstone, Tremp-Graus Basin, northern Spain. *Sedimentary Geology* 229, 9–40.
- Li, Y., Bhattacharya, J.P., Ahmed, S., Garza, D., 2018. Re-evaluating the paleogeography of the river-dominated and wave-influenced Ferron Notom Delta, Southern Central Utah: an integration of detailed facies-architecture and paleocurrent analysis. *Journal of Sedimentary Research* 88, 214–240.
- Liangqing, X., Galloway, W.E., 1991. Fan delta, braid delta and the classification of delta systems. *Acta Geologica Sinica-English Edition* 4, 387–400.
- Lin, W., Bhattacharya, J.R., 2021. Storm-flood-dominated delta: a new type of delta in stormy oceans. *Sedimentology* 68, 1109–1136.
- List, E.J., 1982. Turbulent jets and plumes. *Annual Review of Fluid Mechanics* 14, 189–212.
- Macdonald, H.A., Wynn, R.B., Huvenne, V.A., Peakall, J., Masson, D.G., Weaver, P.P., McPhail, S.D., 2011. New insights into the morphology, fill, and remarkable longevity (>0.2 my) of modern deep-water erosional scours along the northeast Atlantic margin. *Geosphere* 7, 845–867.
- MacNaughton, R.B., Dalrymple, R.W., Narbonne, G.M., 1997. Early Cambrian braid-delta deposits, MacKenzie Mountains, north-western Canada. *Sedimentology* 44, 587–609.
- Martini, I., Sandrelli, F., 2015. Facies analysis of a Pliocene river-dominated deltaic succession (Siena Basin, Italy): implications for the formation and infilling of terminal distributary channels. *Sedimentology* 62, 234–265.
- Martinsen, O.J., 1990. Fluvial, inertia-dominated deltaic deposition in the Namurian (Carboniferous) of northern England. *Sedimentology* 37, 1099–1113.
- Martins-Neto, M.A., Catuneanu, O., 2010. Rift sequence stratigraphy. *Marine and Petroleum Geology* 27, 247–253.
- Massari, F., 1996. Upper-flow-regime stratification types on steep-face, coarse-grained, Gilbert-type progradational wedges (Pleistocene, southern Italy). *Journal of Sedimentary Research* 66, 364–375.
- Massari, F., 2017. Supercritical-flow structures (backset-bedded sets and sediment waves) on high-gradient clinoform systems influenced by shallow-marine hydrodynamics. *Sedimentary Geology* 360, 73–95.
- McPherson, J.C., Shanmugam, G., Muiola, R.J., 1987. Fan-deltas and braid deltas: varieties of coarse-grained deltas. *Geological Society of America Bulletin* 99, 331–340.
- Melstrom, E.M., Birgenheier, L.P., 2021. Stratigraphic architecture of climate influenced hyperpycnal mouth bars. *Sedimentology* 68, 1580–1605.
- Mortimer, E., Gupta, S., Cowie, P., 2005. Clinoform nucleation and growth in coarse-grained deltas, Loreto basin, Baja California Sur, Mexico: a response to episodic accelerations in fault displacement. *Basin Research* 17, 337–359.
- Muhlbauer, J.G., Fedo, C.M., 2020. Architecture of a river-dominated, wave- and tide-influenced, pre-vegetation braid delta: Cambrian middle member of the Wood Canyon Formation, southern Marble Mountains, California, USA. *Journal of Sedimentary Research* 90, 1011–1036.
- Mulder, T., Syvitski, J.P., Migeon, S., Faugeres, J.C., Savoye, B., 2003. Marine hyperpycnal flows: initiation, behavior and related deposits. A review. *Marine and Petroleum Geology* 20, 861–882.
- Mutti, E., Davoli, G., Tinterri, R., Zavala, C., 1996. The importance of ancient fluvio-deltaic systems dominated by catastrophic flooding in tectonically active basins. *Memorie di Scienze Geologiche* 48, 233–291.
- Mutti, E., Tinterri, R., Biase, D., Fava, L., Mavilla, N., Angella, S., Calabrese, L., 2000. Delta front associations of ancient flood-dominated fluvio-deltaic systems. *Revista de la Sociedad Geológica de España* 13, 165–190.
- Mutti, E., Tinterri, R., Benevelli, G., di Biase, D., Cavanna, G., 2003. Deltaic, mixed and turbidite sedimentation of ancient foreland basins. *Marine and Petroleum Geology* 20, 733–755.
- Myrow, P.M., Fischer, W., Goodge, J.W., 2002. Wave-modified turbidites: combined-flow shoreline and shelf deposits, Cambrian, Antarctica. *Journal of Sedimentary Research* 72, 641–656.
- Nemeč, W., 1990. Deltas - remarks on terminology and classification. In: Colella, A., Prior, B.D. (Eds.), *Coarse-Grained Deltas*. International association of Sedimentologists, Special Publication 10, pp. 3–12.
- Nemeč, W., Lonne, I., Blikra, L.H., 1999. The Kregnes moraine in Gaudalen, west-central Norway: anatomy of a Younger Dryas proglacial delta in a paleofjord basin. *Boreas* 28, 454–476.
- Olariu, C., Bhattacharya, J.P., 2006. Terminal distributary channels and delta front architecture of river-dominated deltas. *Journal of Sedimentary Research* 76, 212–233.
- Olariu, C., Steel, R.J., Petter, A.L., 2010. Delta-front hyperpycnal bed geometry and implications for reservoir modeling: Cretaceous Panther Tongue delta, Book Cliffs, Utah. *AAPG Bulletin* 94, 819–845.
- Olariu, C., Zhou, C., Steel, R., Zhang, Z., Yuan, X., Zhang, J., Chen, S., Cheng, D., Kim, W., 2020. Controls on the stratal architecture of lacustrine delta successions in low-accommodation conditions. *Sedimentology* <https://doi.org/10.1111/sed.12838>.

- Ono, K., Plink-Björklund, P., Eggenhuisen, J.T., Cartigny, M.J., 2021. Froude supercritical flow processes and sedimentary structures: new insights from experiments with a wide range of grain sizes. *Sedimentology* 68, 1328–1357.
- Overeem, I., Kroonenberg, S.B., Veldkamp, A., Groenesteijn, K., Rusakov, G.V., Svitoch, A.A., 2003. Small-scale stratigraphy in a large ramp delta: recent and Holocene sedimentation in the Volga Delta, Caspian Sea. *Sedimentary Geology* 159, 133–157.
- Overeem, I., Syvitski, J.P.M., Hutton, E.W.H., 2005. Three-dimensional numerical modeling of deltas. In: Bhattacharya, J.P., Giosan, L. (Eds.), *River Deltas: Concepts, Models and Examples*. Society for Sedimentary Geology, Special Publications 83, pp. 13–30.
- Parsons, J.D., Bush, J.W., Syvitski, J.P., 2001. Hyperpycnal plume formation from riverine outflows with small sediment concentrations. *Sedimentology* 48, 465–478.
- Piliouras, A., Kim, W., Carlson, B., 2017. Balancing aggradation and progradation on a vegetated delta: the importance of fluctuating discharge in depositional systems. *Journal of Geophysical Research - Earth Surface* 122, 1882–1900.
- Plink-Björklund, P., Steel, R.J., 2004. Initiation of turbidity currents: outcrop evidence of hyperpycnal flow turbidites. *Sedimentary Geology* 165, 29–52.
- Postma, G., 1990. Depositional architecture and facies of river and fan deltas: a synthesis. In: Colella, A., Prior, B.D. (Eds.), *Coarse-grained Deltas*. International Association of Sedimentologists, Special Publication 10, pp. 13–27.
- Postma, G., 1995. Sea-level-related architectural trends in coarse-grained delta complexes. *Sedimentary Geology* 98, 3–12.
- Postma, G., Lang, J., Hoyal, D.C., Fedele, J.J., Demko, T., Abreu, V., Pederson, K.H., 2021. Reconstruction of bedform dynamics controlled by supercritical flow in the channel-lobe transition zone of a deep-water delta (Sant Llorenç del Munt, north-east Spain, Eocene). *Sedimentology* 68, 1674–1697.
- Powell, R.D., 1990. Glacimarine processes at grounding-line fans and their growth to ice-contact deltas. In: Dowdeswell, J.A., Scourse, J.D. (Eds.), *Glacimarine Environments: Processes and Sediments*. Geological Society of London, Special Publications 53, pp. 53–73.
- Rajchl, M., Uličný, D., Mach, K., 2008. Interplay between tectonics and compaction in a rift-margin, lacustrine delta system: Miocene of the Eger Graben, Czech Republic. *Sedimentology* 55, 1419–1447.
- Reesink, A.J., Bridge, J.S., 2011. Evidence of bedform superimposition and flow unsteadiness in unit-bar deposits, South Saskatchewan River, Canada. *Journal of Sedimentary Research* 81, 814–840.
- Roberts, P.J., Maile, K., Daviero, G., 2001. Mixing in stratified jets. *Journal of Hydraulic Engineering* 127, 194–200.
- Roberts, H.H., Coleman, J.M., Bentley, S.J., Walker, N., 2003. An embryonic major delta lobe: a new generation of delta studies in the Atchafalaya-Wax Lake delta system. *Gulf Coast Association of Geological Societies Transactions* 53, 690–703.
- Rowland, J.C., Stacey, M.T., Dietrich, W.E., 2009. Turbulent characteristics of a shallow wall-bounded plane jet: experimental implications for river mouth hydrodynamics. *Journal of Fluid Mechanics* 627, 423–449.
- Russell, H.A.J., Amott, R.W.C., 2003. Hydraulic jump and hyperconcentrated-flow deposits of a glacial subaqueous fan: Oak Ridges Moraine, Southern Ontario, Canada. *Journal of Sedimentary Research* 73, 887–905.
- Schomacker, E.R., Kjemperud, A.V., Nystuen, J.P., Jahren, J.S., 2010. Recognition and significance of sharp-based mouth-bar deposits in the Eocene Green River Formation, Uinta Basin, Utah. *Sedimentology* 57, 1069–1087.
- Slootman, A., Cartigny, M.J.B., 2020. Cyclic steps: Review and aggradation-based classification. *Earth-Science Reviews* 201, 102949. <https://doi.org/10.1016/j.earscirev.2019.102949>.
- Slootman, A., Vellinga, A.J., Moscarriello, A., Cartigny, M.J.B., 2021. The depositional signature of high-aggradation chute-and-pool bedforms: the build-and-fill structure. *Sedimentology* 68, 1640–1673.
- Sohn, Y.K., Son, M., 2004. Synrift stratigraphic geometry in a transfer zone coarse-grained delta complex, Miocene Pohang Basin, SE Korea. *Sedimentology* 51, 1387–1408.
- Surlyk, F., Bruhn, R., 2020. Flood-generated hyperpycnal delta front sands of the Brora Arenaceous Formation (upper Callovian–middle Oxfordian) of the Inner Moray Firth, Scotland, record the onset of rifting. *Scottish Journal of Geology* 56, 159–174.
- Tan, C., Plink-Björklund, P., 2021. Morphodynamics of supercritical flow in a linked river and delta system, Daihai Lake, Northern China. *Sedimentology* 68, 1606–1639.
- Turner, J.S., 1986. Turbulent entrainment: the development of the entrainment assumption, and its application to geophysical flows. *Journal of Fluid Mechanics* 173, 431–471.
- Turner, B.R., Tester, G.N., 2006. The Table Rocks Sandstone: a fluvial, friction-dominated lobe mouth bar sandbody in the Westphalian B Coal Measures, NE England. *Sedimentary Geology* 190, 97–119.
- Tuttle, K.J., Øoustmo, S.R., Andersen, B.Ø.G., 1997. Quantitative study of the distributary braidplain of the Preboreal ice-contact Gardermoen delta complex, southeastern Norway. *Boreas* 26, 141–156.
- Tye, R.S., Coleman, J.M., 1989. Evolution of Atchafalaya lacustrine deltas, south-central Louisiana. *Sedimentary Geology* 65, 95–112.
- Uličný, D., 2001. Depositional systems and sequence stratigraphy of coarse-grained deltas in a shallow-marine, strike-slip setting: the Bohemian Cretaceous Basin, Czech Republic. *Sedimentology* 48, 599–628.
- Van den Berg, J.H., Van Gelder, A., Mastbergen, D.R., 2002. The importance of breaching as a mechanism of subaqueous slope failure in fine sand. *Sedimentology* 49, 81–95.
- Van Wagoner, J.C., Hoyal, D.C.J.D., Adair, N.L., Sun, T., Beaubouef, R.T., Deffenbaugh, M., Dunn, P.A., Huh, C., Li, D., 2003. Energy dissipation and the fundamental shape of siliclastic sedimentary bodies. *Search and Discovery*, 40080.
- Van Yperen, A.E., Poyatos-Moré, M., Holbrook, J.M., Midtkandal, I., 2020. Internal mouth-bar variability and preservation of subordinate coastal processes in low-accommodation proximal deltaic settings (Cretaceous Dakota Group, New Mexico, USA). *The Depositional Record* 6, 431–458.
- Vaucher, R., Pittet, B., Humbert, T., Ferry, S., 2018. Large-scale bedforms induced by supercritical flows and wave-wave interference in the intertidal zone (Cap Ferret, France). *Geo-Marine Letters* 38, 287–305.
- Walker, R.G., 1975. Conglomerates: sedimentary structures and facies models. In: Harms, J.C., Walker, R.G., Spearing, D. (Eds.), *Depositional Environments as Interpreted From Primary Sedimentary Structures and Stratification Sequences*. SEPM Short Course Lecture Notes 12, pp. 133–161.
- Wellner, R., Beaubouef, R., Van Wagoner, J., Roberts, H., Sun, T., 2005. Jet-plume depositional bodies – the primary building blocks of Wax Lake Delta. *Gulf Coast Association of Geological Societies Transactions* 55, 867–909.
- Went, D.J., 2020. Fluvial shoal water deltas: pre-vegetation sedimentation through the fluvial-marine transition, Lower Cambrian, English Channel region. *Sedimentology* 67, 330–363.
- Winsemann, J., Hornung, J.J., Meinsen, J., Aspiron, U., Polom, U., Brandes, C., Bußmann, M., Weber, C., 2009. Anatomy of a subaqueous ice-contact fan and delta complex, Middle Pleistocene, north-west Germany. *Sedimentology* 56, 1041–1076.
- Winsemann, J., Lang, J., Polom, U., Loewer, M., Igel, J., Pollock, L., Brandes, C., 2018. Ice-marginal forced regressive deltas in glacial lake basins: geomorphology, facies variability and large-scale depositional architecture. *Boreas* 47, 973–1002.
- Wright, D.L., 1977. Sediment transport and deposition at river mouths: a synthesis. *Geological Society of America Bulletin* 88, 857–868.
- Wynn, R.B., Kenyon, N.H., Masson, D.G., Stow, D.A.V., Weaver, P.P.E., 2002. Characterization and recognition of deep-water channel-lobe transition zones. *AAPG Bulletin* 86, 1441–1462.
- Zavala, C., 2020. Hyperpycnal (over density) flows and deposits. *Journal of Palaeogeography* 9, 17. <https://doi.org/10.1186/s42501-020-00065-x>.
- Zavala, C., Ponce, J.J., Arcuri, M., Dritanti, D., Freije, H., Asensio, M., 2006. Ancient lacustrine hyperpycnites: a depositional model from a case study in the Rayoso Formation (Cretaceous) of West-Central Argentina. *Journal of Sedimentary Research* 76, 41–59.
- Zhu, X., Zeng, H., Li, S., Dong, Y., Zhu, S., Zhao, D., Huang, W., 2017. Sedimentary characteristics and seismic geomorphologic responses of a shallow-water delta in the Qingshankou Formation from the Songliao Basin, China. *Marine and Petroleum Geology* 79, 131–148.